Petrology and Geochemistry of Low- SiO_2 adakites Quaternary Volcanic Rocks in the West of Kohin, East of Qorveh (Northwest of Iran)

Mohammad Ali Salimizand[1]*, Robab Hajialioghli[1], Mohsen Moayyed[1], Ahmad Jahangiri[1]

1- a Department of Earth Sciences, Faculty of Natural Sciences, University of Tabriz, Tabriz, Iran

*Corresponding author: mohamadalisalimizand@gmail.com (Mohammad Ali Salimizand)

Abstract: This study presents in combination with petrography, Microprobe analysis of minerals, major and trace element geochemistry and Sr, Nd, Pb radiogenic isotope data in order to characterize and discuss the origin of volcanic rocks in Case Study. In the northern part of the Sanandaj- Sirjan Zone (SSZ), northwestern Iran, in the west of Kohin, east of Qorveh there are a number of young (0.339- 0.112 Ma) dismembered volcanic complexes that extend parallel to the Zagros Suture Zone in a northwest– southeast direction. The major lithologies associated with these complexes Trachy andesite, andesite, dacite. These rocks display microlitic to porphyritic textures with plagioclase, pyroxene, amphibole as phenocrysts. These rocks are characterized by Na_2O (3.5-7.5wt %) and low Y (<18), high Sr (>400), high Sr/Y (>40) and La/Yb (>25) ratios. Initial $^{87}Sr/^{86}Sr$ ratios are relatively of high (0.7064–0.7066). Major and trace element bulk rock geochemistry and initial Sr, Nd, Pb radiogenic isotope data on the rocks provide new constraints on the Quaternary volcanism in this region. Analyses of chemical compositions confirm that these rocks belong to the low silica adakite group. The Sr–Nd ratios, Isotope ratios of Pb and also geochemistry studies indicate that the samples of the study area are located near the crust and these rocks are from continental crust derived from partial melting and suggest that the parent magma originated from melting of the crust after continental collision.

Keywords: volcanic rocks, adakite, geochemistry, Quaternary, west of Kohin, Sanandaj-Sirjan

1- Introduction

In the 1970s, adakites were said to be rocks that were formed on the edge of converging structures from the melting of hot and young oceanic crust (less than 25 million years) (Kay, 1978). The geochemical characteristic of these rocks is the high amount of Al, Ba, Sr and the high proportion of Sr/Y, La/Yb. But today, adakite is called a large group of rocks that have high Sr/Y and La/Yb levels So it can be said that Adakites are characterized by high Sr/Y and La/Yb ratios and, in comparison with normal calc-alkaline rocks, are enriched in light rare earth elements (LREEs) and are depleted in high field strength elements (HFSEs) and heavy rare earth elements (HREEs) (Defant and Drummond, 1990, Defant et al., 1991, Rapp et al., 1991). This feature is due to processes such as melting of subducted oceanic crust, melting of origin rich in Sr, La and Y and poor in Yb, Y, melting in deep areas with garnet left behind, crystal separation and reaction of felsic lava with the mantle (Martin et al., 2005). Defant and Drummond (1990) proposed that these rocks originated from the partial melting of oceanic slabs in the garnet- amphibolites or eclogite facies. Other researchers have since proposed a variety of sources, including flux mixing of slab fluid or with the mantle, melting of metasomatized at

 https://doi.org/10.5281/zenodo.14858968

high pressure, lower continental crustal melting during or after collision and melting of hot oceanic slabs during flat subduction (e.g., Atherton and Petford, 1993; Yogodzinski et al., 1995; Hou et al., 2004; Chung et al., 2003; Kamei et al., 2009; Chiaradia, 2009; Jahangiri, 2007). Adakites are common extensional in subduction, collision and regimes, although their distribution is not limited to active zones (Castillo, 2012). The identification of adakites and their genesis research is important from two aspects, one is due to the special tectonic and thermal regimes according to which these compounds are created and the other is due to the association of most adakite compounds with copper, molybdenum and gold deposits in Connection with porphyry or no connection with it (Li et al., 2007). The topic of Adakity is very new in Iran, and only in the last few years, a few reports of such a combination have been published in magazines like Jahangiri, (2007), Azizi et al. (2013) and etc. Jahangiri (2007) first reported the presence of adakites in north-western Iran. Several researchers have since described adakites along the Urumiah Dokhtar Magmatic Arc (UDMA) and Zagros volcanic belt in the western and central parts of Iran (Agard et al., 2011; Ghorbani and Bezanjani, 2011). Most of these studies have proposed that adakites in Iran were produced by oceanic slab melting beneath the Sanandaj- Sirjan Zone (Central Iran) and partial melting of the crust during or after The Arabian-Iranian plate collision. Nearby in Turkey and the Caucus region, many granitic and volcanic rocks with adakite and adakite- like compositions have been reported (Varol et al., 2007; Topuz et al., 2011; Karsli et al., 2010; Eyuboglu et al., 2011). Of course, it should be noted that it is possible that a number of factors – such as slab melting, flat subduction of a hot slab, crustal melting and magma differentiations – may have played essential roles in producing different types of adakite in this belt. This paper will investigate the origin of adakites in the northern part of the Sanandaj- Sirjan Zone (SSZ), northwestern Iran, in the west of Kohin, east of Qorveh on the basis of chemical compositions ratios and isotope.

2- Geological background

Adakitic rocks in the Alpine-Himalayan belt are indicative for the geodynamic evolution of collision zones and often associated with mineralization. Adakites can provide information about magmatic processes, crustal evolution, and ore deposit formation at convergent margins. Their identification is important to constrain the fate of the oceanic slab during subduction and the processes of crustal recycling at convergent margins (Castillo 2006). The ultimate sources and causes of partial melting to form these mag-mas in a post-collisional setting are debated. The Iranian plateau is part of the Alpine-Himalayan belt orogenic and is divided into eight main structural deep zones separated by faults (Stocklin and Nabavi, 1972). A large variety of post-collisional igneous rock of adakitic, calc-alkaline, ultra-potassic, and alkaline affinity has been documented for northwestern Iran (e.g., Ja-hangiri 2007, Ahmadzadeh et al. 2010, Dabiri et al. 2011, Lechmann et al. 2018, Faridazad 2020). The Sanandaj-Sirjan Zone (SSZ) is situated between the Zagros in the west and the Urumieh-Dokhtar Volcanic belt in the east. The SSZ can be divided into distinct northern and southern sections (Ghasemi and Talbot, 2006; Azizi and Moinevaziri, 2009). Azizi and Asahara (2013) showed is that the northern section is mainly composed of an old island arc and an active continental margin that collided in the Late Jurassic–Early Cretaceous. The Southern section consists entirely of metamorphic basement with evidence of poly-deformation and poly-metamorphism, although metamorphic grade decreases to the

 https://doi.org/10.5281/zenodo.14858968

intruded north. The SSZ has been primarily by typical S- and I-type granites between the Jurassic and Tertiary periods (e.g., Sepahi and Athari, 2006; Shahbazi et al., 2010; Mansouri Esfahani et al., 2010). In the northern section, basalts and basaltic andesites outcrop between Zagros Thrust Fault and the Tabriz Fault and are frequently with Cretaceous shales, Sandstones and calcareous rocks. This volcanic complex is completely calc-alkaline and was formed in an active continental margin Setting (Azizi and Jahangiri, 2008). In the northern Section of the SSZ, dismembered volcanic complexes extend in a northwest–southeast direction parallel to Zagros Fault (Fig. 1); Azizi and Moinevaziri (2009) termed this area the Hamadan-Tabriz Volcanic belt (HTV). The HTV is mainly composed of acidic rocks and the degree activity increases northward. Volcanic rocks in the Dehgolan and Bijar areas have been described by Boccaletti et al. (1976) as mostly calc-alkaline and high in potassium. Richards et al. (2006) described the volcanic rocks in the Sari Gunay area (15 km east of the study area) as calc-alkaline and proposed that these rocks formed after the Arabian-Iranian plate collision. The Mesozoic to Present geology of Iran largely results from subduction of the Tethys Ocean and subsequent collision between Arabia and Eurasia, which began in late Eocene- early Oligocene times (e.g. Berberian and King, 1981). Subduction and collision generated magmatic arcs and the Turkish-Iranian Plateau (Şengör and Kidd, 1979) which is largely covered by Mid- Miocene to Quaternary volcanic rocks. A large variety of Neogene magmas such as adakitic, ultrapotassic and alkaline basaltic magmas has been documented for Iran (Fig, 1 and 2) and (table, 1). Adakitic magmas reported in Azerbaijan and the central part of the UDMA (Jahangiri, 2007; Omrani et al., 2008) were interpreted as melts of a detached Neotethyan slab. At variance, Pang et al. (2016) inferred that the adakitic compositions in the central UDMA are rather generated by lower crustal melting. The studie area is located in the southwestern end of Kohin between Kurdistan and Hamadan provinces are divided into Intermediate rocks. The Intermediate rocks extend direction in a northwest– southeast. They are generally black and entirely smooth and are composed of lava. According to the field studies, such as the location of the units of the studied area on the lahar (late Pliocene age) (Khan Nazer et al, 2014), the Intermediate rocks of the studied area are of Quaternary age. We found in that The Intermediate rocks region are very fresh, with extremely limited Alteration dating to the Quaternary (Based on field and isotope studies) (Fig 3).

3- Analytical methods

After sampling and field visit of various samples of the studied area, thin sections and polished thin sections were prepared and then these sections were studied by polarizing microscope. After conducting detailed petrographic studies, the samples with the least amount of weathering and alteration were selected for chemical analysis of main, secondary and rare earth elements. After this stage, the samples were subjected to analysis of microprobes minerals in the study area that the samples were analyzed in the laboratory (Wuhan Sample Solution Analytical Technology Co., Ltd.) in China. Minerals microprocessor device of JXA-8230 type and 15Kv voltage test conditions and COMPO signal type are used. The results of these analyzes were used in the rock geochemistry studies of the studied rock units and also elemental analysis was done by ICP-OES method in the laboratory of ICAS company in China. In order to detect the weight and atomic percentage of some elements such, the scanning electron microscope method (EDX) was used, which was carried out in the

 https://doi.org/10.5281/zenodo.14858968

laboratory of ICAS in China (FOV: 179μm, Mode: 15kV-Detector :BSDFull). Then, the samples were subjected to chemical analysis of whole rock. In the laboratory (Wuhan Sample Solution Analytical Technology Co., Ltd., China), We determined the chemical compositions Elements of major and trace using an X-ray fluorescence (XRF) Spectrometer (ZSX Primus II) in the Wuhan Sample Solution Analytical Technology Co, Ltd in China. We measured the Abundances of rare earth elements (Agilent (REEs)) using an ICP-MS 7700e (ptima Perkin Elmer 4000 Series), also at Wuhan Sample Solution Analytical Technology Co, Ltd in China. In the laboratory (Wuhan Sample Solution Analytical Technology Co., Ltd., China), In addition to the analysis of microprobes minerals in the study area, For the Nd, Pb and Sr isotope analyses, all preparation steps have been carried out with high precision, such as: Choosing the right sample that was made from healthy stones without any weathering, and then the samples were washed and dried with ethanol and the samples were placed inside plastic bags to avoid any contact with hands and other particles, and the samples were crushed in a completely clean environment, and in the next step, the samples were crushed to below 250 microns, and the samples were transferred into special storage containers, without any direct contact with hands. And after that, the sample label containing the name, project name and date was inserted on it, then the samples were prepared for dissolution and in order to dissolve the samples of the studied area from concentrated hydrofluoric acid (37% HF) was used. Then, about 100 mg of sample powder was weighed by a precise scale and transferred into Teflon containers (Beaker), and in the next step, 0.5 to 1 ml of acid ($HCLO_4$) was added to the sample. Of course, before adding concentrated acid to the sample, it was placed under an acid-resistant hood, and then concentrated acid was added to the samples, and in the next step, 2 to 3 ml of concentrated hydrofluoric acid (37% HF) was added again. It was added gradually on each sample. In the next step, the samples were placed on a hot plate with a temperature of 125-140 degrees Celsius for 48 hours, and then, by maintaining the temperature, two infrared lamps were placed on the samples until the samples To dry, this process took about 3 days. After drying the samples, 6 ml of hydrochloric acid was added to the samples and they were placed in a centrifuge with a speed of about 3000 for 15 minutes, then the plastic tubes were separated from the centrifuge and separated. Clear solution (Suppernant) was transferred to a suitable container and it was transferred again on a (Hot Plate) without a cover to dry completely, and then 0.2 ml of concentrated percaloric acid and 1 ml of concentrated fluoric acid were added and they were transferred inside the Steal Jacket and placed at a temperature of about 180 degrees Celsius, and then the samples were dried at a temperature of 140-120 degrees and also using an infrared lamp until the entire sample dry, and in the next step, dividing the samples according to the purpose of isotopic analysis was done on the samples, and then drying the samples, adding concentrated nitric acid and drying the samples again. And in the next step, a drop of concentrated nitric acid is added to dissolve the sample well, and then the sample is re-washed using nitric acid with a concentration of 2% in three steps and transferred to P.S bottles. The data and weighing of the samples have been done, as well as the purification process, which is done using special resins that have great power in absorbing and repelling elements based on the concentration of different acids, and then in the machine (MC-ICP-MS) was placed.

 https://doi.org/10.5281/zenodo.14858968

4- Petrography and mineral compositions

The adakites studied here are crystallized from lava. They usually have relatively large phenocrysts and intermediate minerals and in the manual sample, the color of the samples is generally pale to light grey and contains Phenocrysts on field descriptions and microscopic can observations, they be classified generally into intermediate groups such andesite, trachyte andesite, dacite (Fig. 4 a–f). Under the microscope the most common textures are micro porphyritic ,sive textur, glomeroporphyric. Phenocrysts are mostly plagioclase and Consist mainly hornblende, Pyroxene. The plagioclases are zoned and structure commonly exhibit sieve in the center of the grain. Pyroxenes are among the minerals of the other sections studied. This mineral can be seen in two forms: orthopyroxene and clinopyroxene. But clinopyroxenes are more abundant than orthopyroxenes. Zoning is observed in some plagioclase of the studied area. In the studied andesites, amphiboles are observed in a spindle-shaped cross-section. Sanidine is observed as one of the constituent minerals of trachian andesitic rocks in some sections. (Fig. 5 a–f). The results of microprobe analysis of plagioclase of the studied samples change in the compositional range between late labradorite (An: 60) in the margin to late bitonite (An: 78) in the center (Table 2, Fig. 6 a and b). Pyroxene mineral is also seen in the studied sections. The existing clinopyroxenes are often shaped to semi-shaped and can be distinguished by one set of faces in longitudinal sections and two sets of perpendicular faces in transverse sections. Orthopyroxene microphenocrysts occur as euhedral and subhedral crystals. The results of microprobe analysis of the studied clinopyroxenes are Quad (Fe-Mg-Ca)-type and are placed in the the diopside range and the orthopyroxenes of the studied area are also in the range of enstatite (Table 3 and 4, Fig. 6 c and d,). According to the criteria for classifying amphiboles (Leake et al, 1997), the amphiboles of the studied samples are in the realm of clastic amphiboles, which can be characterized by the parameters (Na <0.5 and B(Ca+ Na) ≥ 1 and ≥ 1.5 (CaB~). Also in Below this group in the graph of the ratio of Mg/(Mg+Fe+2) versus silicon, there are amphiboles of the (Mg-Hornblende) type (Table 4, Figure 6 e and f). The thermometry of orthopyroxenes in the studied area shows an average temperature of 1250 degrees Celsius for pressures of 2 to 8 kbar. This thermometry was performed using the relationship (Kohler & Brey, 1990).

5. Geochemistry

To examine the geochemistry and tectonic setting of the volcanic rocks in the West of Kohin, East of Qorveh (Northwest of Iran), we complement our results with data presented Chemical analyses for major and trace elements for the intermediate rocks in the case study area (see table the 5 and 6). In the adakitic samples, SiO_2 ranges shown in table 6 that the From 59/05 to 63.79 wt% and the Al_2O_3 levels are high range from 16/74 to 18.52 wt%, the Na_2O/K_2O the ratios are >0.9, and MgO value ranges from 0.28 to 1/49, Sr wt.% the high amounts of (865–1214 ppm), low amounts of Y (<20 ppm) and Yb (<2 ppm), Sr/Y Ratios (57–123) and high enrichments elements of LILE and LREE (Rb, Ba, Cs, La and Ce) (table, 6). In the diagram comparing SiO_2 with alkali elements (Le Bas al., 1986), the adakitic samples plot in the trachyte, trachy dacite, andesite, trachy andesite fields (Fig. 7a). In the diagram (Peccerillo and Taylor, 1976, comparing SiO_2 and K_2O), samples sub alkaline plot in the high-K calc-series range (Fig. 7b).

 https://doi.org/10.5281/zenodo.14858968

ISSN: 0369-8963

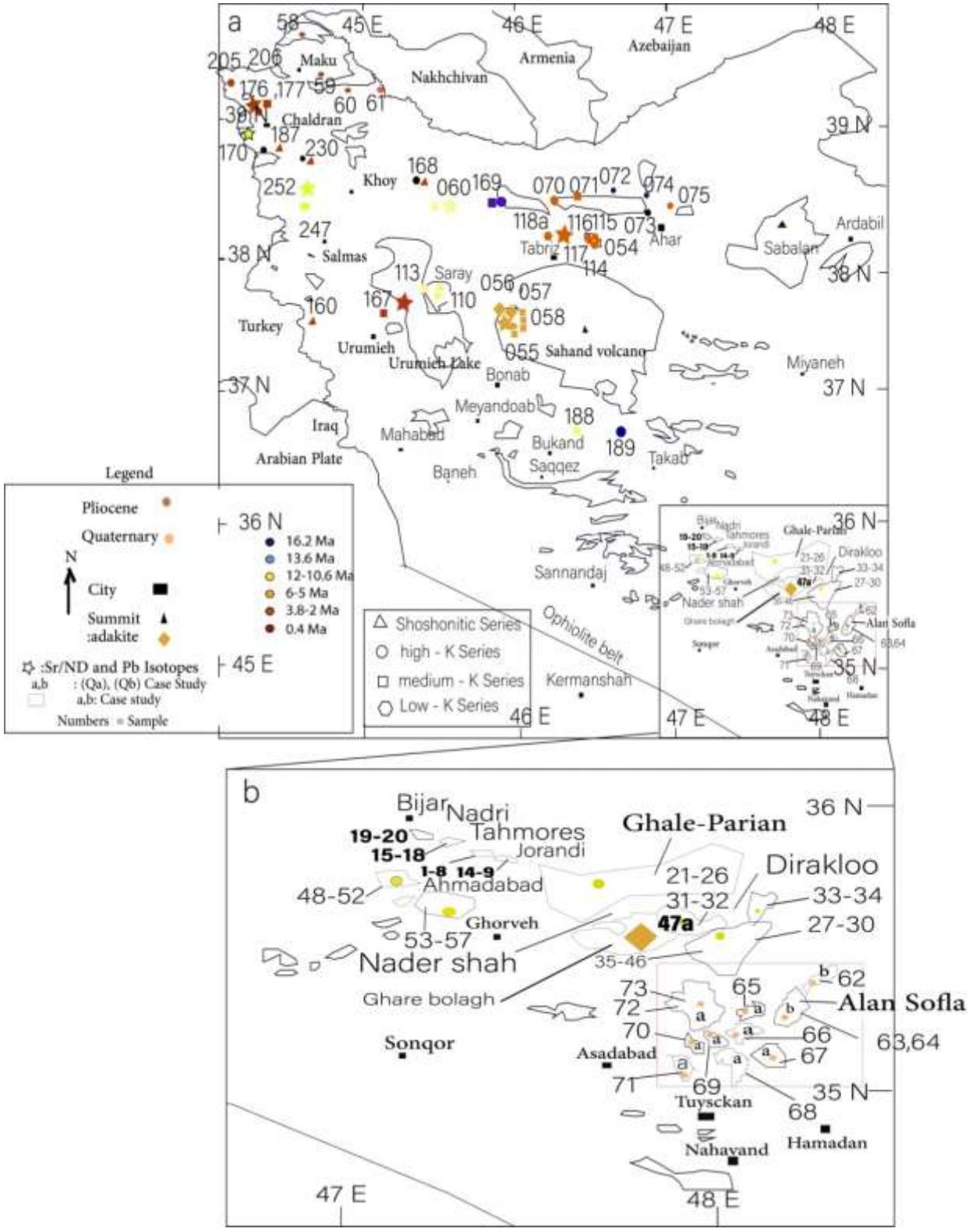

Fig. 1. Comparison of the sampling sites of the study area and neighboring areas based on age (ages are indicated by color codes) and (black dots are without age), age determination based on isotopic ratios (Sr, Nd, Pb) and ($^{40}Ar/^{39}Ar$) are given, the numbers and sources are given in Tables 1, based on (Lechmann et al 2018 with changes)

https://doi.org/10.5281/zenodo.14858968

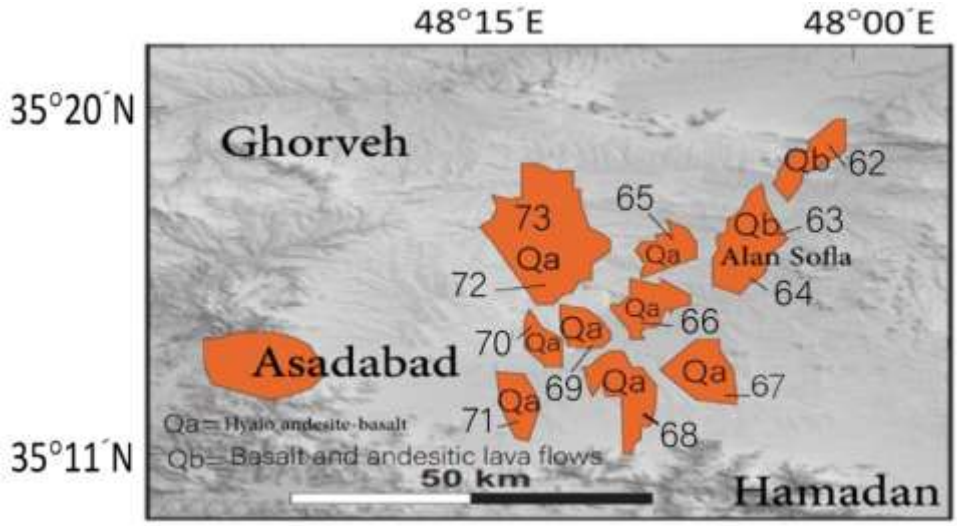

Fig. 2. The location of the rocks of the studied area with neighboring areas

Table. 1. Comparison of the samples of Fig 1 in terms of magmatic series and tectonic environment, along with the sources used

Sample, Position	Series- $^{206}Pb/^{238}U$, $^{40}Ar/^{39}Ar$ (Ma) ages (†:Field studies)	Tectonic- Name according to TAS
1-20 (razavi et al, 2009) (Southeastern Bijar)	Alkaline-sub alkalis, (1- 8 Miosen†), (9- 20 PLQ)	WPB, Alkali basalt, Huawit, Mojarite, Trachy- andesite
21-36 (azizi et al, 2014 (A)) (northern Ghorveh)	high alkalis- (PLQ)†	OIB, Basalt, Trachy-andesite, Dacite
37-46 (Shikh zakeriaei et al, 2014) (northeast of Ghorve)	Alkaline- Quaternary†	WPB, Basalt,Olivine basalt,andesite basalt
47a (Koohbanani, et al, (2017)) (Northeast Ghorveh)	Alkaline -Quaternary†	WPB -Basalt, Andesite basalt,Andesite, Trachy-andesite
48-57 (Azizi et al, 2014 (B)) (Ghorveh)	Adakites (High- k calc- alkaline)- 10 ±11 ($^{40}Ar/^{39}Ar$ metod)	Acm, Rhyolite, Trachy-dacite, Dacite
58-61 (Allen et al, 2011) (northwest Iran)	Alkaline-sub alkalis - Quaternary†	Acm - Andesite
054-058, 060, 070, 070-075, 110, 113-117, 118a, 160, 167-170, 176, 177, 187-189, 206, 207, 230, 247, 252 (Lechmann et al, 2018)- (northwest Iran)	100,168,230,187,110,170(Shoshonitic).247, 252, 070, 206, 075, 189, 116, 176(High-k)- 2.75 ± 0.07 (206Pb/238U method).075,169,071,167,176,058,055,056,057,188(Medium-k), ± 0.07 (206Pb/238U method). 060, 117, 114, 118a, 054, 115 (Low-k), ± 0.07 ($^{206}Pb/^{238}U$ method)	post-collision: Dacitic, rhyolite, Trachydacite, Trachy andesite, Alkali-basalt
62-73 (This study)	Adakites (High- k calc- Alkaline)	post-collision: Trachy andesite, andesite, dacite

Finally, in diagrams comparing Sr/Y with Y, all samples plot the adakite field (Fig. 7 c). Based on the silica content in the rock, Martin and Moyen (2005) introduced two types of adakite magmas, one rich in silica (HSA) and the other with low silica (LSA), which are respectively associated with adakites Identified by (Defant and Drummond, 1990) and magnesium-bearing andesites (Kay, 1978). These two adakite groups are different in terms of mineralogical, geochemical and petrogenesis characteristics (Fig. 7 d). The pattern of minor elements normalized to the primary mantle of adakites is unique to this group as well as other geochemical characteristics. In order to confirm the adakites of the studied area belong to the low silica adakites group introduced by Martin et al (2005), the spider diagram pattern of

 https://doi.org/10.5281/zenodo.14858968

ISSN: 0369-8963

this rock group was compared with the low silica adakites (LSA) of that classical article. (Fig. 8 a and b). The result significantly reveals the belonging of these adakites to the mentioned group. The pattern of the spider diagram of these two groups is completely similar. The difference between HSA and LSA, more than mineralogical or chemical differences, reflects fundamental differences in petrogenesis and specifically in the melt source. The HSA type is a direct result of the melting of subducting Hydate basalts, which melt is contaminated with digested peridotites in different proportions during ascent from the mantle wedge (Martin et al., 2005). Low-silica types of Nb and the total content of rare earth elements are higher (Figure 8 a and b) (Martin et al., 2005). Isotopic ratios in adakites of the study area were also investigated. Adakites often show a high ratio of Sr isotope and a low ratio of Nd isotope (Aguillón-Robles et al., 2001) (Fig. 9). In Figure 10, the isotope ratios of Nd and Sr are given against the key ratios of adakites from Kolb et al. (2003) and the samples of the studied area are also marked on it.

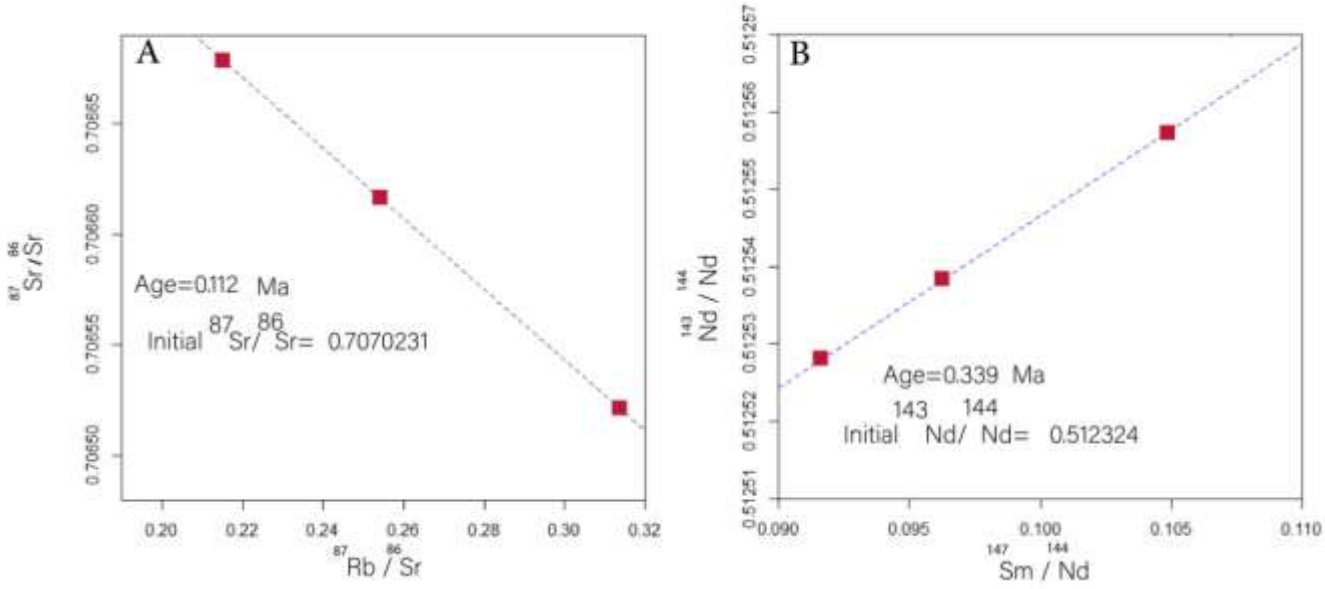

Fig. 3. Isochron diagrams based on isotopic ratio data, Fig A) $^{87}Rb/^{86}Sr$ versus $^{87}Rb/^{86}Sr$ diagram, where the initial value of $^{87}Sr/^{86}Sr$ ratio is equal to 0.7070231 and shows an age equal to 0.112 million years ago. Fig B) $^{147}Sm/^{144}Nd$ versus $^{143}Nd/^{144}Nd$ graph, where the initial value of the $^{147}Sm/^{144}Nd$ ratio is it shows 0.512324 and an age equal to 0.339 million years ago.

6. Discussion

The variability of volcanic formations such as lava flows and domes belong to Quaternary volcanic rocks. The adakites samples of the studied area have characteristics such as SiO_2 > 56 wt%, Al_2O_3 > 15 wt%, high amounts of Na_2O (Na_2O<7.5), K_2O/Na_2O ratio low (~0.42), Sr values are high, LILE is high and HREE is low which is the characteristics of adakites (Castillo, 2006; Martin, 1999; Defant and Drummond, 1990).

 https://doi.org/10.5281/zenodo.14858968

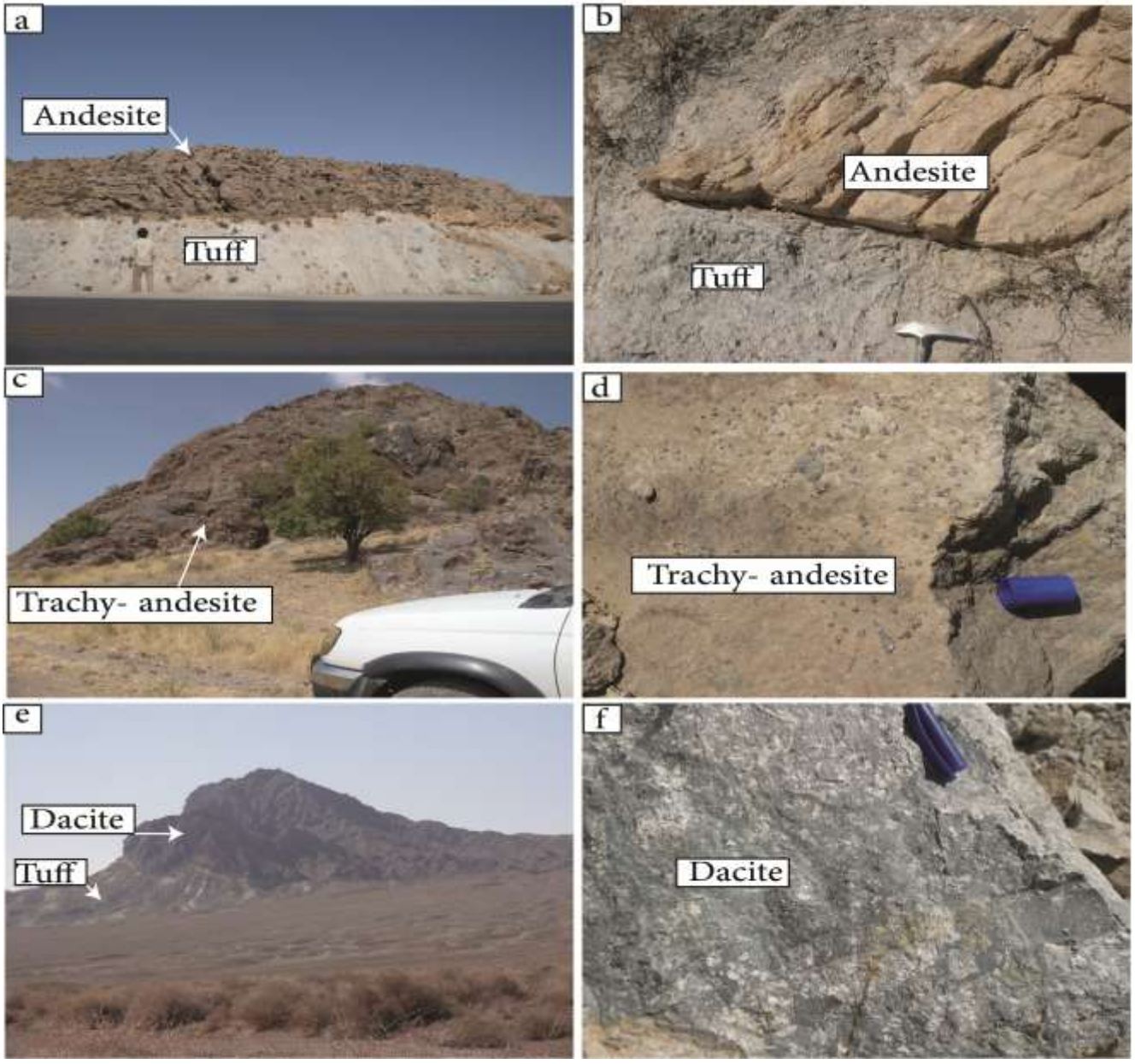

Fig. 4. Field photographs of selected rocks from the case studty; a) the placement of a rock unit with the composition of andesite of Quaternary age on the lahar (with lower Pliocene age) with the composition Tuff, around the northwest of Bharlo, looking towards the east b) A close-up view of the samples related to this unit in the desert.c) Prospect of Trachy andesite units of Quaternary age, near In Guzel Abdal area, looking east. d) Close-up of samples related to trachy andesite e) dacite units in the around the northwest of Bharlo, looking towards the east f) Close-up of samples related to dacite units.

According to (Castillo, 2006), adakites are used to define internal and external igneous rocks rich in silicates with high Sr/Y and La/Yb ratios, which are formed as a result of partial melting of the oceanic crust. Subducting under the volcanic arc is used in young subduction zones, and according to (Prouteu et al, 2001), adakite is a type of acidic magma rich in water, which under steam pressure conditions the water is formed.

https://doi.org/10.5281/zenodo.14858968

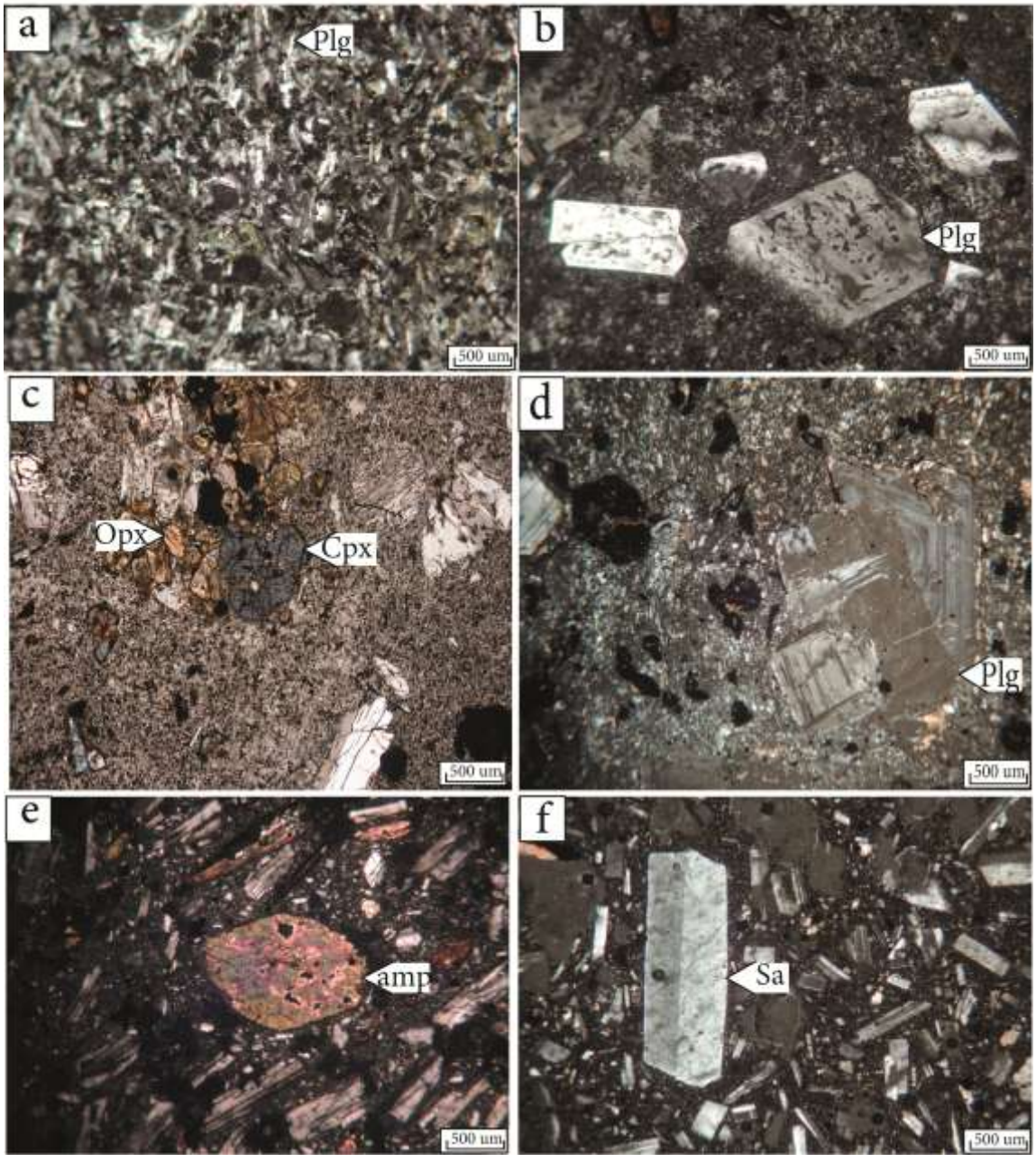

Figure 5 a) Texture micro porphyritic in andesites of the studied area b) Sieve Texture in plagioclase, in dacite in studied area c) Accumulation of orthopyroxene along with clinopyroxene and texture glomeroporphyric in andesites case study d) Zoning in plagioclase, in dacite case study e) amphibole in andesites studied area f) Sanidine mineral in trachy andesites of the studied area.

According to (Defant & Drummond, 1990), most adakites contain MgO less than 3% by weight, so the compositional range of adakite rocks is from siliceous magma derived from melting of young subducting basaltic crust to Mg-rich andesitic magmas produced through the equilibration of these siliceous magmas are altered with mantle-wedge peridotite (Defant & Drummond, 1990).

 https://doi.org/10.5281/zenodo.14858968

ISSN: 0369-8963

Table 2. The results of the microprobe analysis of plagioclase the calculation of their structural formula (the structural formula of plagioclase is calculated based on 8 oxygen) (By: Bytownite, La: Labradorit)

	Mi-29-1-Q1 (Andesite)					Mi-29-1-Q4 (Trachy andesite)					Mi-28-1-Q1 (Dacite)					Mi-28-1-Q2 (Andesite)				
	3	4	5	2	1	8	9	10	7	6	13	14	15	12	11	3	2	1	4	5
	C	R C	R	RC	R	C	RC	R	RC	R	C	RC	R	RC	R	C	RC	R	RC	R
SiO_2	49.1	50.1	50.9	49.5	47.7	49.9	50.7	52.3	50.7	53	51.2	50.3	49.8	51.3	51.1	49.7	48.3	50.1	50.6	50.2
TiO_2	0	0	0.03	0.03	0.04	0	0.02	0.01	0.01	0	0.02	0	0.08	0.06	0.05	0.01	0.04	0.05	0.03	0.03
Al_2O_3	32	31.2	30.4	32	33	32	31	29	31	29	30.2	3.31	32.3	30.1	30.9	31.8	32.2	30.6	31	31.3
FeO	0.52	0.59	0.55	0.57	0.51	0.49	0.63	0.51	0.49	0.52	0.60	0.68	0.62	0.52	0.51	0.58	0.55	0.65	0.48	0.60
MnO	0.03	0	0	0	0	0	0	0	0	0	0	0	0.03	0	0	0	0	0	0	0
MgO	0	0	0.06	0.02	0.01	0.06	0.07	0.05	0.06	0.06	0.05	0.04	0.04	0.09	0.06	0.02	0.04	0.06	0.04	0.09
CaO	15	14.2	13.7	14.4	16.1	14.6	13.5	12.8	13.8	12.3	12.8	14	14.5	13.2	12.6	14.7	15.8	14.1	13.9	14.3
Na_2O	2.77	2.93	3.25	2.72	2.13	2.92	3.26	3.81	3.26	4.23	3.50	3.12	2.84	3.53	3.65	2.82	2.29	3.30	3.09	3.01
K_2O	0.24	0.30	0.36	0.22	0.16	0.24	0.34	0.38	0.35	0.49	0.43	0.25	0.24	0.32	0.38	0.23	0.18	0.32	0.26	0.29
Cr_2O_3	0.01	0	0	0	0	0	0	0	0.03	0	0	0/03	0	0.05	0	0	0	0	0	0.01
ZnO	0	0	0.03	0	0	0.13	0.01	0.02	0	0.04	0	0	0	0	0	0.02	0	0	0	0.04
NiO	0	0	0	0.02	0.02	0	0	0	0	0	0.01	48	0.01	0.03	0	0	0.01	0	0	0
BaO	0	0.01	0.10	0	0.04	0.07	0.07	0.10	0.09	0	0.02	0	0.05	0	0.01	0	0.03	0	0	0.05
Total	99.9	99.4	99.5	99.7	100	100	100	99.8	100	100	98.9	99.8	100	99.3	99.4	100	99.5	99.3	99.5	100
Si	9.02	9.20	9.35	9.07	8.77	9.08	9.26	9.54	9.22	9.62	9.42	9.21	9.06	9.42	9.36	9.10	8.91	9.42	9.27	9.19
Ti	0	0	0	0	0	0	0	0	0	0	0	0	0.01	0	0	0	0	0	0	0
Al	6.92	6.76	6.58	6.93	7.18	6.90	6.72	6.40	6.76	6.30	6.55	6.75	6.92	6.51	6.66	6.86	7.01	6.65	6.69	6.75
Fe(ii)	0.08	0.09	0.08	0.08	0.07	0.07	0.09	0.07	0.07	0.08	0.09	0.10	0.09	0.08	0.07	0.08	0.08	0.10	0.07	0.09
Ca	2.96	2.79	2.69	2.83	0.07	2.85	2.65	2.50	2.70	2.39	2.53	2.75	2.83	2.61	2.47	2.88	3.12	2.79	2.73	2.80
Na	0.98	1.04	1.15	0.96	3.18	1.03	1.15	1.34	1.15	1.48	1.24	2.75	1	1.25	1.29	1	0.81	1.18	1.10	1.06
K	0.05	0.07	0.08	0.05	0.75	0.05	0.08	0.08	0.08	0.11	0.10	0.05	0.05	0.07	0.09	0.05	0.04	0.07	0.06	0.06
Ab	24.6	26.6	29.4	25	19	26.1	29.7	34.1	29.2	37.2	32.1	28.3	25.7	31.8	33.6	25.3	20.5	29.1	28.2	27.1
An	73.8	71.4	62.4	73.5	65	72.3	63.1	63.5	68.6	59.8	75.2	70.1	62.7	66.2	64	73.2	78.3	62.9	61.1	60.1
Or	1.45	1.85	2.15	1.35	1	1.46	2.09	2.27	2.07	2.88	2.61	1.51	1.48	1.93	2.33	1.36	1.10	1.87	1.61	1.76
Name	La	Byt	La	By	La	By	La	La	La	La	By	By	La	La	La	By	By	La	La	La

https://doi.org/10.5281/zenodo.14858968

ISSN: 0369-8963

Table 3 results of microprobe analysis of pyroxenes along with the calculation of their structural formula

	Mi-29-1-Q4 (Trachy andesite)					Mi-29-1-Q5-CPX (Trachy andesite)					Mi-29-1-Q3 (Dacite)					Mi-28-1-Q1 (Dacite)				
	3	2	1	4	5	3	2	1	4	5	3	2	1	4	5	3	2	1	4	5
	C	RC	R	RC	R	C	RC	R	RC	R	C	RC	R	RC	R	C	RC	R	RC	R
SiO2	50.2	51.7	51.1	50.3	51.3	51.2	51.5	51.2	50.7	51.6	52	50.8	50.4	51.2	51.1	51.5	51.6	51.6	51.5	51.4
TiO2	0.78	0.43	0.59	0.76	0.50	0.65	0.58	0.53	0.6	0.63	0.56	0.63	0.78	0.52	0.68	0.55	0.55	0.57	0.52	0.53
Al2O3	3.48	1.98	2.46	3.26	1.97	2.56	2.40	2.46	3.20	2.39	2.15	3.17	3.58	2.72	2.93	2.35	2.21	2.30	2.19	2.17
FeO	10.8	11.1	10.3	11.1	10.8	10.5	9.69	10.5	10.3	10.9	10.3	10	10.7	9.64	9.66	10.6	11.1	10.2	10.8	11
MnO	0.44	0.41	0.42	0.46	0.44	0.38	0.35	0.39	0.33	0.44	0.38	0.36	0.36	0.35	0.36	0.42	0.45	0.41	0.43	0.44
MgO	13.4	13.8	14	13.3	13.8	13.7	14.3	13.8	13.9	14	13.9	13.7	13.2	14.1	13.9	14	14	14.3	14	13.9
CaO	19.9	19.7	19.8	19.3	19.7	19.9	19.6	19.7	20	20	19.9	20.2	19.8	20	20.2	19.5	19	19.8	19.5	19.7
Na2O	0.3	0.27	0.26	0.28	0.24	0.26	0.26	0.27	0.27	0.28	0.29	0.25	0.29	0.22	0.27	0.23	0.25	0.30	0.25	0.27
K2O	0	0	0	0	0	0	0/01	0	0	0	0	0	0	0	0	0	0	0	0	0
P2O5	0.01	0.02	0	0.03	0	0	0.01	0	0	0	0	0.02	0.01	0.04	0	0	0	0	0.02	0.01
NiO	0	0.02	0	0.02	0.03	0.01	0	0	0.02	0.01	0.03	0.02	0	0	0.04	0	0	0.02	0.01	0.04
Cr2O3	0	0	0	0/01	0	0	0	0	0	0	0	0	0/02	0	0/01	0	0	0	0/03	0
Total	99.5	99.7	99.2	99	99	99	98.9	99.1	99.5	100	99.7	99.3	99.2	98.9	99.2	99.4	99.4	99.6	99.4	99.6
Si	1.89	1.94	1.92	1.90	1.94	1.92	1.94	1.93	1.90	1.92	1.94	1.91	1.90	1.93	1.92	1.93	1.94	1.93	1.93	1.93
Ti	0.02	0.01	0.01	0.02	0.01	0.01	0.01	0.01	0.01	0.01	0.01	0.01	0.02	0.01	0.01	0.01	0.01	0.01	0.01	0.01
Al	0.15	0.08	0.10	0/14	0.08	0.11	0.10	0.11	0.14	0.10	0.09	0.14	0.15	0.12	0.13	0.10	0.09	0.10	0.09	0.09
Fe+3	0.04	0.01	0.02	0.02	0.01	0.01	0	0.01	0.04	0.03	0	0/02	0.01	0	0.01	0	0	0.02	0.01	0.02
Cr+3	0	0	0	0	0	0	0	0	0	0	0	0	0	0	0	0	0	0	0	0
Fe+2	0.29	0.33	0.30	0.33	0.32	0.31	0.30	0.31	0.28	0.31	0.32	0.29	0.32	0.29	0.29	0.33	0.34	0.29	0.32	0.32
Mg	0.75	0.77	0.78	0.75	0.78	0.77	0.80	0.77	0.78	0.77	0.78	0.76	0.74	0.79	0.78	0.78	0.79	0.80	0.78	0.77
Mn	0.01	0.01	0.01	0.01	0.01	0.01	0.01	0.01	0.01	0.01	0.01	0.01	0.01	0.01	0.01	0.01	0.01	0.01	0.01	0.01
Ca	0.80	0.79	0.80	0.78	0.80	0.80	0.79	0.79	0.80	0.79	0.80	0.81	0.80	0.80	0.81	0.78	0.76	0.79	0.78	0.79
Na	0.02	0.02	0.01	0.02	0.01	0.01	0.02	0.02	0.02	0.02	0.02	0.01	0.02	0.01	0.02	0.01	0.01	0.02	0.01	0.02
K	0	0	0	0	0	0	0	0	0	0	0	0	0	0	0	0	0	0	0	0
S-cat	4	4	4	4	4	4	4	4	4	4	4	4	4	4	4	4	4	4	4	4
WO	43.3	41.7	42.3	41.9	42	42.4	41.6	42.1	43	42.3	41.9	43.3	42.8	42.4	43.1	41.2	40.3	42.2	41.3	41.8
EN	40.6	40.7	41.7	40.2	40.9	40.6	42/2	41.1	41.7	41.2	40.9	40.9	39.7	41.8	41.4	41.3	41.4	42.3	41.4	41.1
Fs	16	17/.5	15.9	17.7	17	16.8	16	16.7	15.1	16.4	17	15.8	17.4	15.6	15.4	17.3	18.2	15/4	17.1	16.9
Mg#	0.71	0.70	0.72	0.69	0.70	0.70	0.72	0.71	0.73	0.71	0.70	0.72	0.69	0.72	0.72	0.70	0.69	0.73	0.70	0.70

https://doi.org/10.5281/zenodo.14858968

Table 3. continued

	Mi-28-1-Q2 (Andesite)					Mi-28-1-Q2 (Andesite)					Mi-29-1-Q3-CPX (Dacite)					Mi-29-1-Q5-CPX (Trachy andesite)				
	3	2	1	4	5	8	7	6	9	10	3	2	1	4	5	3	2	1	4	5
	C	RC	R	RC	R	C	RC	R	RC	R	C	RC	R	RC	R	C	RC	R	RC	R
SiO_2	50	50.1	49.8	50.1	49.9	51.6	50.8	51.4	51.4	51.1	51.2	51.4	51.6	51.1	50.9	51.2	51.5	51.2	50.7	51.6
TiO_2	0.83	0.79	0.88	0.62	0.71	0.56	0.67	0.50	0.50	0.51	0.59	0.54	0.49	0.55	0.61	0.65	0.58	0.53	0.60	0.63
Al_2O_3	5.05	3.84	4.45	3.82	4.02	2.86	2.87	2.31	2.39	1.98	2.76	2.50	2.13	2.58	2.78	2.56	2.40	2.46	3.20	2.39
FeO	8.53	10.2	9.88	9.38	9.52	11	10.4	10.4	10.3	12.8	10.5	10.4	10.4	10.4	10.3	10.5	9.69	10.5	10.3	10.9
MnO	0.24	0.35	0.25	0.30	0.30	0.42	0.34	0.41	0.41	0.47	0.41	0.40	0.39	0.40	0.44	0.38	0.35	0.39	0.33	0.44
MgO	14	13.7	13.4	13.7	13.5	15.2	13.9	14.2	14.2	12.9	13.6	13.9	14	14	13.5	13.7	14.3	13.8	13.9	14
CaO	20.8	19.7	20.3	20.4	20.6	17.7	19.9	19.9	20	19.2	19.8	19.9	19.5	19.9	20	19.9	19.6	19/7	20	20
Na_2O	0.23	0.31	0.28	0.30	0.30	0.21	0.24	0.27	0.29	0.23	0.22	0.32	0.25	0.26	0.28	0.26	0.26	0.27	0.27	0.28
K_2O	0	0	0	0	0	0	0	0	0	0	0/01	0	0	0	0	0	0/01	0	0	0
P_2O_5	0	0.01	0.02	0.04	0.01	0.02	0	0.01	0.02	0.01	0.01	0.01	0	0.01	0.01	0	0.01	0	0	0
NiO	0	0	0.01	0.03	0	0	0.01	0	0	0	0	0	0	0	0.02	0.01	0	0.01	0.02	0.01
Cr_2O_3	0.09	0.12	0.03	0.05	0.06	0	0	0	0	0.02	0.01	0	0	0	0.02	0	0	0	0	0
Total	99.9	99.4	99.3	98.9	99.2	99.9	99.4	99.6	99.7	99.4	99.3	99.5	98.9	99.0	99.0	99.4	98.9	99.4	99.5	100
Si	1.85	1.88	1.87	1.88	1.87	1.92	1.90	1.92	1.91	1.94	1.92	1.92	1.94	1.92	1.92	1.92	1.94	1.93	1.90	1.92
Ti	0.02	0.02	0.02	0.01	0.02	0.01	0.01	0.01	0.01	0.01	0.01	0.01	0.01	0.01	0.01	0.01	0.01	0.01	0.01	0.01
Al	0.22	0.17	0.19	0.17	0.17	0.12	0.12	0.10	0.10	0.08	0.12	0.11	0.09	0.11	0.12	0.11	0.10	0.10	0.14	0.10
Fe^{+3}	0.03	0.03	0.03	0.04	0.04	0	0.03	0.03	0.06	0.01	0	0.02	0	0.03	0.01	0.01	0	0.01	0.04	0.03
Cr^{+3}	0	0	0	0	0	0	0	0	0	0	0	0	0	0	0	0	0	0	0	0
Fe^{+2}	0.23	0.28	0.27	0.25	0.25	0.34	0.29	2.29	0.28	0.39	0.32	0.30	0.33	0.29	0.31	0.31	0.30	0.31	0.28	0.30
Mg	0.77	0.76	0.75	0.77	0.76	0.84	0.78	0.71	0.78	0.73	0.76	0.78	0.79	0.78	0.76	0.77	0.80	0.77	0.78	0.77
Mn	0	0.01	0	0.01	0.01	0.01	0.01	0.01	0.01	0.01	0.01	0.01	0.01	0.01	0.01	0.01	0.01	0.01	0.01	0.01
Ca	0.83	0.79	0.81	0.82	0.83	0.71	0.80	0.79	0.79	0.78	0.80	0.80	0.78	0.80	0.81	0.80	0.79	0.79	0.80	0.79
Na	0.01	0.02	0.02	0.02	0.02	0.01	0.01	0.02	0.02	0.01	0.01	0.02	0.01	0.01	0.02	0.01	0.02	0.02	0.02	0.02
K	0	0	0	0	0	0	0	0	0	0	0	0	0	0	0	0	0	0	0	0
S-cat	4	4	4	4	4	4	4	4	4	4	4	4	4	4	4	4	4	4	4	4
WO	45.1	43	44.2	44.6	45.1	37.4	42.7	42.2	42.6	41	42.2	42.4	41.2	42.5	43	42.4	41.6	42.1	43	42.3
EN	42.1	41.5	40.7	41.6	41.2	44.6	41.6	42.1	42.1	38.4	40.4	41.5	41.4	41.7	40.3	40.6	42.2	41.1	41.7	41.2
Fs	12.7	15.4	15	13.7	13.6	17.9	15.6	15.5	15.1	20.5	17.3	15.9	17.3	15.7	16.6	16.8	16	16.7	15.1	16.4
Mg#	0.76	0.72	0.73	0.75	0.75	0.71	0.72	0.70	0.73	0.65	0.70	0.72	0.70	0.72	0.70	0.70	0.72	0.71	0.73	0.71

https://doi.org/10.5281/zenodo.14858968

ISSN: 0369-8963

In general, today, adakites are a large group of rocks that have high Sr/Y and La/Yb levels, and this feature is due to processes such as melting of the subducted oceanic crust, molten of origin rich in La and poor in Y and Yb melting in deep areas with garnet, crystalline separation and reaction of felsic lava with the mantle have occurred (Martin et al., 2005). Other researchers consider potassic rocks with a high Sr/Y ratio to be continental adakites, which result from various petrogenesis processes (Defant & Drummond, 1990; Morris, 1990; Martin, 1999). Common mineral phases in adakites often include zoned plagioclase phenocrysts, hornblende. The rocks of the studied area are in the range of adakites. In general, low-silica adakites and high-silica adakites are formed in subduction-related environments and when the subducting lithosphere is hot and young (Defant & Drummond, 1990; Morris, 1990; Martin, 1999). But today it is known that adakites can be thickened by partial melting of the lower crust or fractional crystallization (Defant et al., 2002; Kay and Kay, 2002; Chung et al., 2003; Castillo, 2006; Wen et al., 2008; Goss and Kay, 2009). These two groups of magmas can be distinguished by geochemical discriminators such as La/Yb and Sr/Y ratios, MgO and Na_2O content. In order to determine the origin of adakitic melts in the studied area, the graph of K_2O/Na_2O against Yb was used (Kamvonget al. 2014) (Fig. 11). Therefore, the adakites of the studied area are of the type contaminated with crust or of crustal origin. In the plot of Nb/Ta vs. Nb from (Rudnick et al. (2000) (Fig. 12), the samples are very close to the upper crustal headquarters. The crustal data Upper UC from Plank (2005), C ratio means the ratio in chondrite, DM is the symbol of depleted mantle and PM is the symbol of primary mantle. Using the partial ratio of elements (Th/Yb versus Ta/Yb graph) (Pearce, 1982), it was found that the samples of the studied area have a composition very close to the average of the upper crust (Fig. 13). The samples are very close to the headquarters of the upper crust. Also, using the graph of Sr against K_2O/Na_2O (Kamei et al., 2009: Eyuboglu et al., 2011) in Figure 14 shows that the adakites of the area the study originates from the melting of the thick crust in the collision zone.

Table 4 results of microprobe analysis of Orthopyroxenes along with the calculation of their structural formula and results of microprobe analysis of amphiboles along with the calculation of their structural formula

Mi-28-1-BU-OPX (Dacite)						Mi-29-1-BU-AMP					
	C	RC	R	RC	R		C	RC	R	RC	R
point	3	4	5	2	1	point	3	4	5	2	1
SiO_2	51.9	51.1	51.9	51.7	52.1	SiO_2	46.4	45.8	45.1	45.8	45.3
TiO_2	0.40	0.31	0.34	0.32	0.46	TiO_2	1.14	1.32	1.21	1.32	1.49
Al_2O_3	0.49	0.51	0.59	0.52	0.59	Al_2O_3	6.16	6.19	6.56	5.94	6.14
FeO	24.1	24.8	24.4	24.1	24.3	FeO	14.2	14.8	14.7	14.8	14.4
MnO	0.92	0.97	0.88	0.93	0.91	MnO	0.27	0.36	0.37	0.29	0.35
MgO	17.9	17.5	17.2	17.7	17.4	MgO	14.2	13.7	13.9	13.6	13.7
CaO	3.92	4.24	4.11	3.58	4.13	CaO	11.2	11	11	11.1	10.8
Na_2O	0.06	0.04	0.06	0.06	0.02	Na_2O	1.86	2.36	2.08	2.23	2.20
K_2O	0.05	0.04	0.03	0.06	0	K_2O	1.16	1.05	1.17	1.10	1.17
P_2O_5	0	0.12	0.01	0	0	P_2O_5	0	0	0	0.01	0
NiO	0	0	0	0	0.01	Cr_2O_3	0	0	0.02	0	0
Cr_2O_3	0	0.02	0	0	0.02	F	1.77	1.57	1.55	1.58	1.58
Total	99.8	99.9	99.7	99.1	100	Cl	0.24	0.22	0.23	0.19	0.20
Si	1.98	1.95	1.99	1.98	1.99	Total	98	97.9	97.4	97.4	96.9

https://doi.org/10.5281/zenodo.14858968

Table 4. continued

Mi-28-1-BU-OPX (Dacite)						Mi-29-1-BU-AMP					
	C	RC	R	RC	R		C	RC	R	RC	R
point	3	4	5	2	1	point	3	4	5	2	1
Ti	0.01	0	0.01	0	0.01	Si	6.85	6.81	6.72	6.85	6.80
Al	0.02	0.02	0.02	0.02	0.02	AlIv	1.07	1.08	1.15	1.04	1.08
Fe^{+3}	0	0/04	0	0	0	Site T	7.92	7.90	7.87	7.90	7.89
Cr^{+3}	0	0	0	0	0	Al (vi)	0	0	0	0	0
Fe^{+2}	0.76	0.75	0.78	0.77	0.77	Ti	0.12	0.14	0.13	0.14	0.16
Mg	1.02	1	0.98	1.01	0.99	Fe(ii)	1.10	1.25	1.05	1.34	1.20
Mn	0.03	0.03	0.02	0.03	0.03	Fe(iii)	0.65	0.59	0.78	0.51	0.60
Ca	0.16	0.17	0.16	0.14	0.16	Mn	0.03	0.04	0.04	0.03	0.04
Na	0	0	0	0	0	Mg	3.14	3.05	3.09	3.04	3.08
K	0	0	0	0	0	Cr	0	0	0	0	0
S-cat	4	4	4	4	4	Site C	5.07	5.09	5.12	5.09	5.10
WO	8.24	9.05	8.71	7.60	8.71	Ca	1.77	1.75	1.75	1.78	1.74
EN	52.4	51.9	50	52.3	51.2	Na	0.22	0.24	0.24	0.21	0.25
Fs	39.3	38.9	40.4	40	40	Site B	2	2	2	2	2
Mg#	0.57	0.57	0.55	0.56	0.56	Na	0.31	0.43	0.35	0.21	0.38
						K	0.21	0.20	0.22	0.21	0.22
						Site A	0.53	0.63	0.58	0.64	0.61

Adakites have special geochemical characteristics. Therefore, this characteristic seems to have been created by several phenomena, such as the presence of garnet in the origin (low Y), the absence of plagioclase in the remaining slag and its participation in melting (high Sr and Sr/ High Y) as mentioned before, high ratio of Sr/Y, La/Yb and LREE/HREE are characteristics of adakite. Negative anomaly of Nb and Ta along with low Y, Sc and HREE may be controlled by garnet and amphibole (Davidson et al, 2013). Garnet and amphibole are essential residual phases in adakites. The negative correlation between Dy/Yb ratio and SiO_2 shows that the residual amphibole was more important than the role of garnet in the production of adakitic melts (Davidson et al, 2013). It can be said that amphibole is an important controller on the contents of moderate REEs during partial melting or during recrystallization of magma. In amphibole, the ratio of Dy/Yb decreases with the increase of SiO_2 found, while in garnet this ratio increases, the samples of the studied area have a negative correlation between Dy/Yb and SiO_2, which shows that amphibole is a single phase. The main residue is during melting (Fig. 15 a and b). According to the experimental results (Kay et al. 1999), amphibole decomposes at a depth of 40 to 50 km. In addition, the ratios of different REEs such as La/Yb, La/Sm and Sm/Yb provide important information about the mineralogy of the origin of the residual melts. It presents the adakity and relative thickness of the shell (Davidson et al, 2013). The diagram of La/Yb versus La (Gao et al, 2007) shows that partial melting is more important than recrystallization during the production of rocks in the studied area (Fig. 16). In general, low ratios of La/Yb (<20), La/Sm (<4) and Sm/Yb (<3) show residual clinopyroxene, in While higher proportions of such elements indicate that heavy REEs such as (Yb) are retained by garnet and amphibole in the residue (Kay et al. 1991, Haschke et al. 2002, Haschke & Günther, 2003, Karsli et al. 2019). Based on the La_N/Yb_N versus Yb_N plot (Martin, 1986), the volcanic rocks of the study area could have been formed by the melting of 10% of the amphibolite garnet source (Fig. 17). However, it should be noted that the negative anomaly of Ti (one of the three components of TNT elements) in the samples of the studied area can also be a

 https://doi.org/10.5281/zenodo.14858968

ISSN: 0369-8963

characteristic of marginal melts (continental or oceanic arc) and also the reason is the influence of the continental crust (as a melting source) from the subduction components (Pearce, 1996).

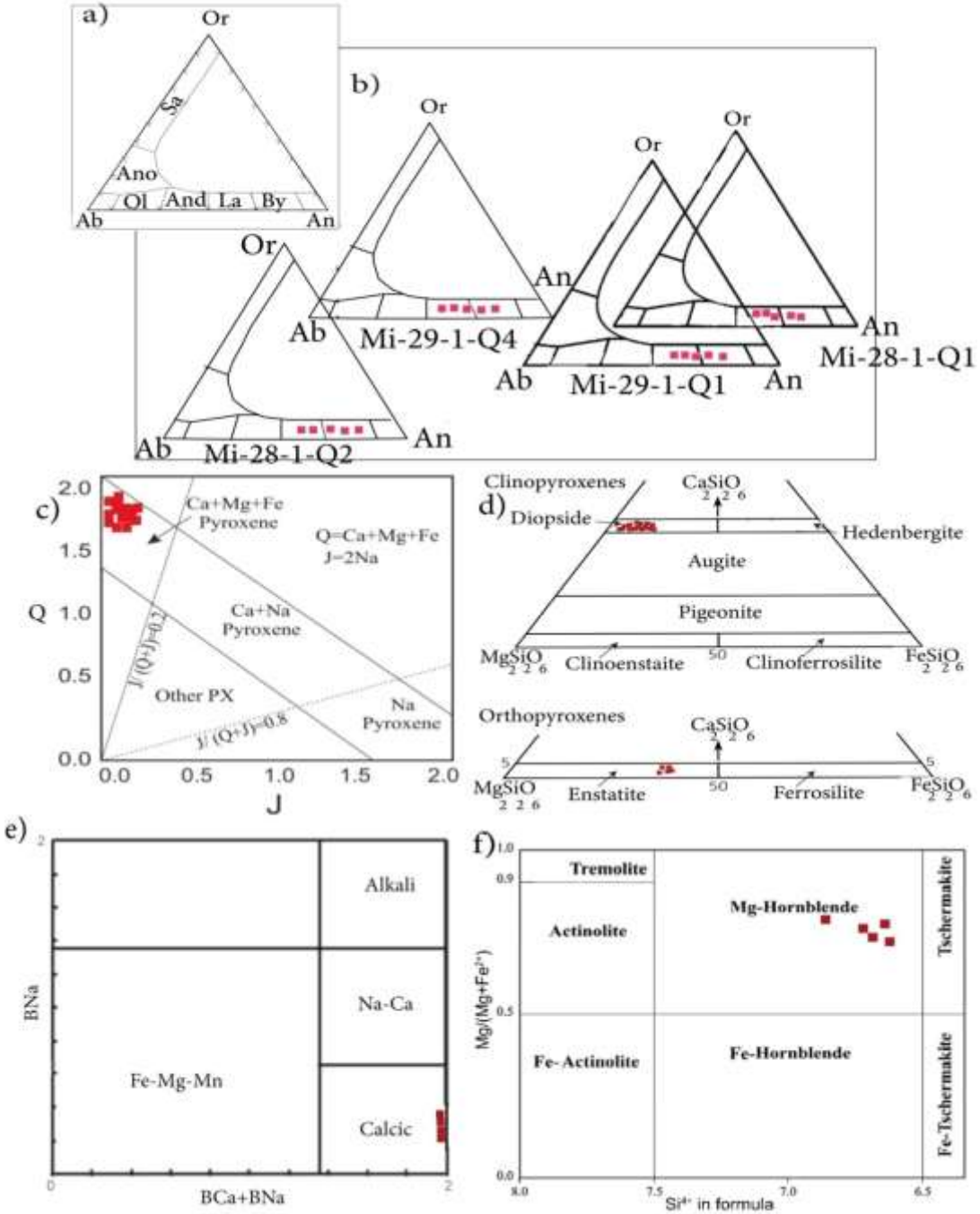

Figure 6 a) ternary diagram of feldspars distribution b) feldspars of the studied area in the composite range of labradorite (An: 60) in the center to Bitonite (An: 78) changes in the margin c) Binary graph of J=(2Na) versus Q=(Ca+Mg+Fe) on which the clinopyroxenes of the studied area are identified (Morimoto, 1988). In this diagram, the studied samples are located in the Quad range, d) distribution diagram of Ca-Mg-Fe pyroxenes (Morimoto, 1989). The clinopyroxenes of the studied area are in the diopside part and the orthopyroxenes are in the enstatite part e) Classification of amphiboles in the rocks of the study area (Leake et al, 1997). e) BCa+BNa vs. BNa graph, the amphiboles of the studied samples are in the realm of clastic amphiboles f) Mg/(Mg+Fe+2) ratio graph In contrast to silica, amphiboles are of the (Mg-Hornblende) type.

 https://doi.org/10.5281/zenodo.14858968

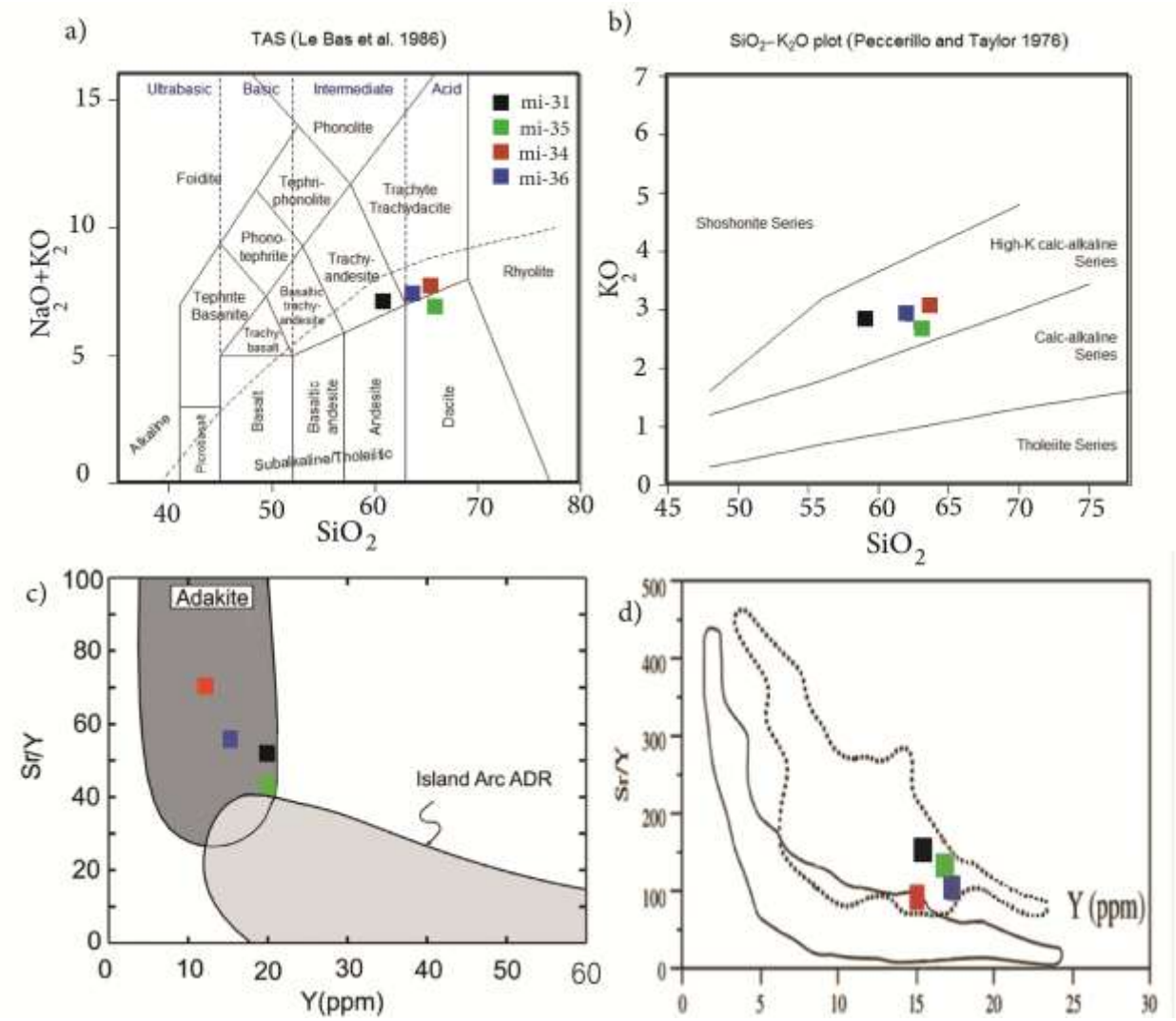

Figure 7 a) Classification diagram of SiO_2 (wt %), versus Na_2O + K_2O (wt%) (Le Bas et al., 1986), with samples plotted in the, andesite, trachy dacite and dacite fields b). Classification SiO_2 versus K_2O (Peccerillo and Taylor, 1976), with samples plotted in the calc-alkaline series field high-K c) Y ratio chart against Sr/Y (Defant and Drummond, 1990: Rapp et al. ., 1991) on which the samples of the studied area are identified and show the characteristics of adakite. d) diagram Y against Sr/Y, where the samples of the studied area are placed in the adakite part with low silica (diagram from Martin et al., 2005) (Symptoms are as in Figure 7 a).

This negative anomaly is attributed to various factors, which include:

1- The characteristic of magmatism related to the subduction process (Sunders et al., 1980) 2- The characteristic of continental crust rocks in magmatic processes (Kuster and Harms, 1997). 3- The sign of the poverty of these elements in the origin is the stability of the phases of these elements during partial melting or their separation during the subtraction process (Rollinson, 1993). In general, more accurate results can be obtained with isotope studies. In Table 9, the data of isotopic analysis of radiogenic elements Rb-Sr and Sm-Nd in the rocks of the studied area based on the average age of 0.225 million years ago (based on Figures 3 a and b).

 https://doi.org/10.5281/zenodo.14858968

ISSN: 0369-8963

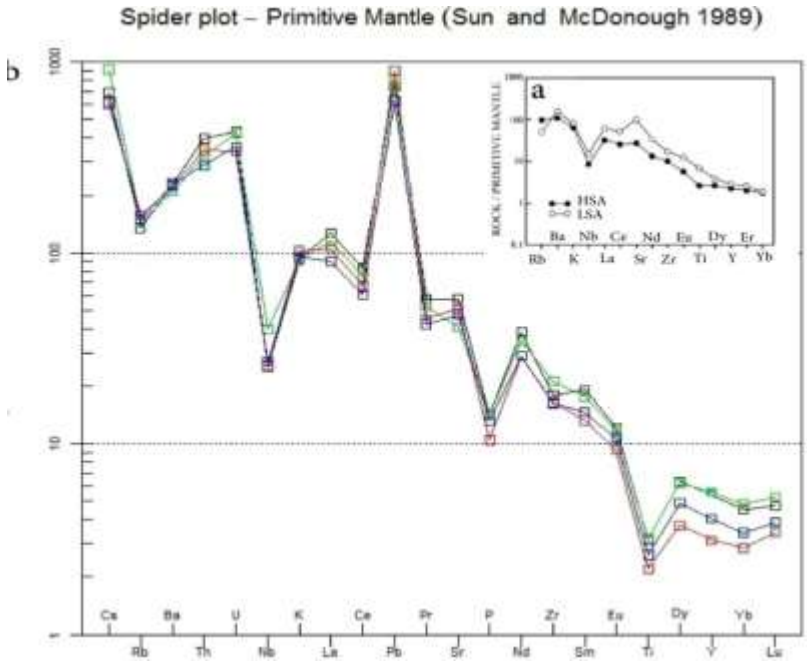

Figure 8: The normalized pattern of minor elements relative to the primary mantle to distinguish low-silica and persiliceous adakites, a) comparison of the spider diagram pattern of low-silica adakite (LSA) with persiliceous adakites (HSA). (Introduced by the article (Martin et al., 2005), b) Spider diagram pattern of low-silica adakite (LSA) of the study area, which has higher niobium and total content of rare earth elements than the types has persilis (HSA). (Symptoms are as in Figure 7 a).

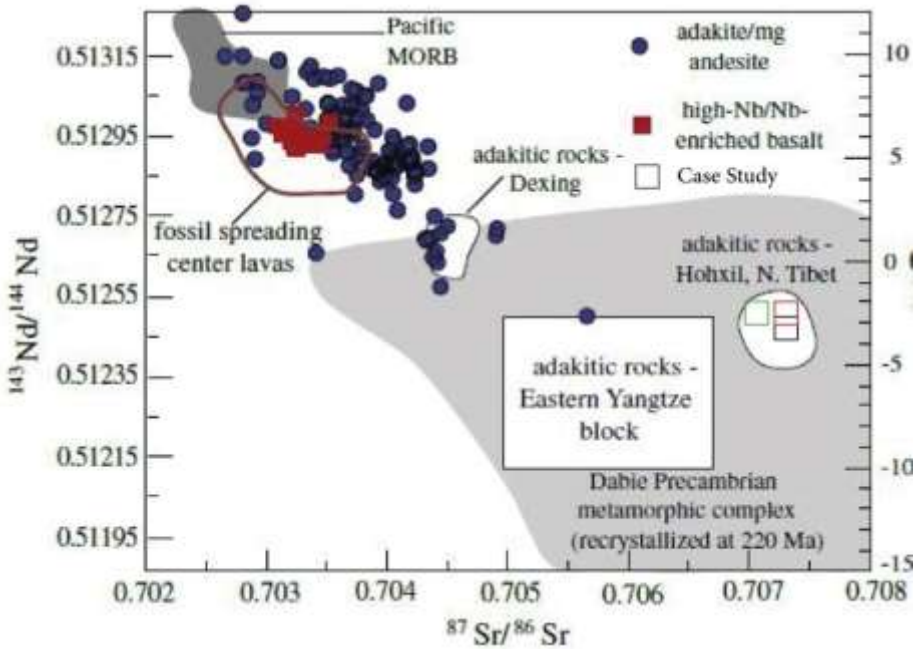

Figure 9: The ratio of $^{87}Sr/^{86}Sr$ against $^{143}Nd/^{144}Nd$ of some Phanerozoic adakites and magnesian andesites (Aguillón-Robles et al., 2001; Danyushevsky et al., 2008; Defant et al., 1992; Martınez-Serrano, 2004; Yogodzinski et al., 1995). Also, some reported adakites (Wang et al., 2004, 2005; Xu et al., 2002) and the Dobshan metamorphic complex of China (Ma et al., 1998) as the reference is given and the samples of the studied area are marked on it.

 https://doi.org/10.5281/zenodo.14858968

ISSN: 0369-8963

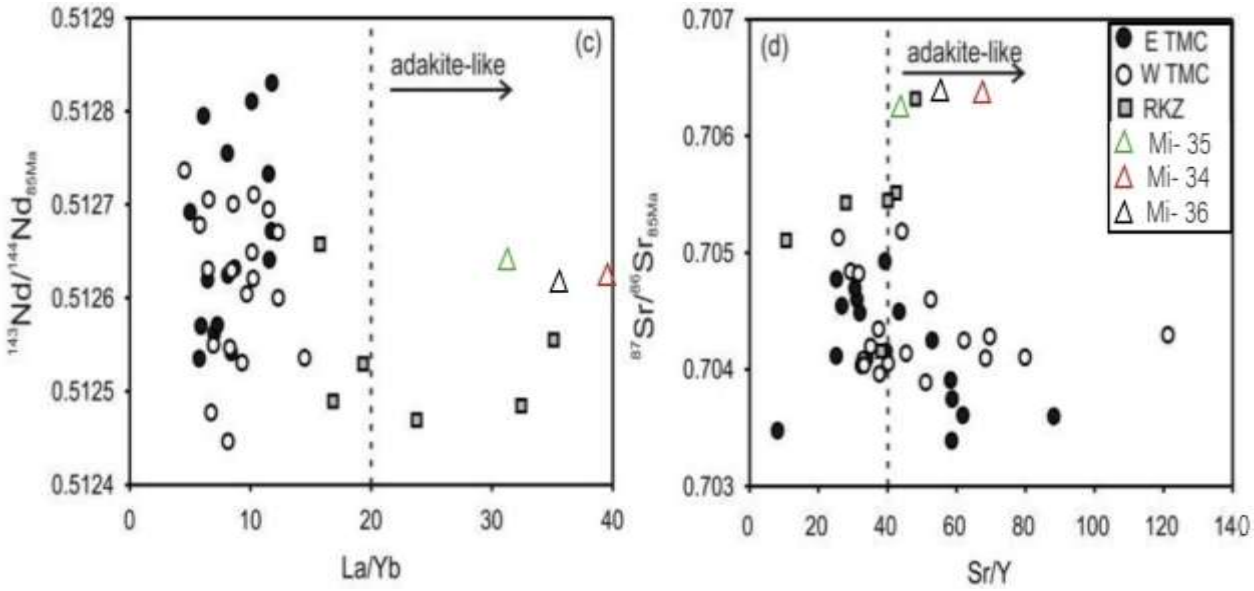

Figure 10 c and d) isotope ratios of Nd and Sr against the key ratios of adakites from (Kolb et al. (2003)), where the data related to the Balkan-Carpathian arc in eastern Siberia and the boundary line of adakites is obtained from (Castillo et al. (1999). The samples of the studied area are marked on it.

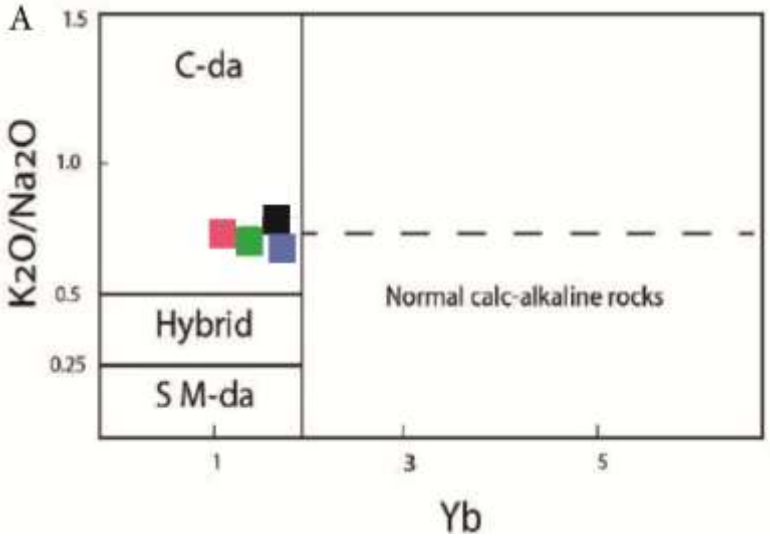

Figure 11, K_2O/Na_2O versus Yb graph to distinguish the origin of adakites (Kamvonget al. 2014). C-da represents adakite derived from continental crust, Hybrid represents dual origin, and SM-da represents adakite derived from oceanic crust melts. Therefore, the adakites of the studied area are of the type contaminated with crust or of crustal origin. (Symptoms are as in Figure 7 a).

 https://doi.org/10.5281/zenodo.14858968

ISSN: 0369-8963

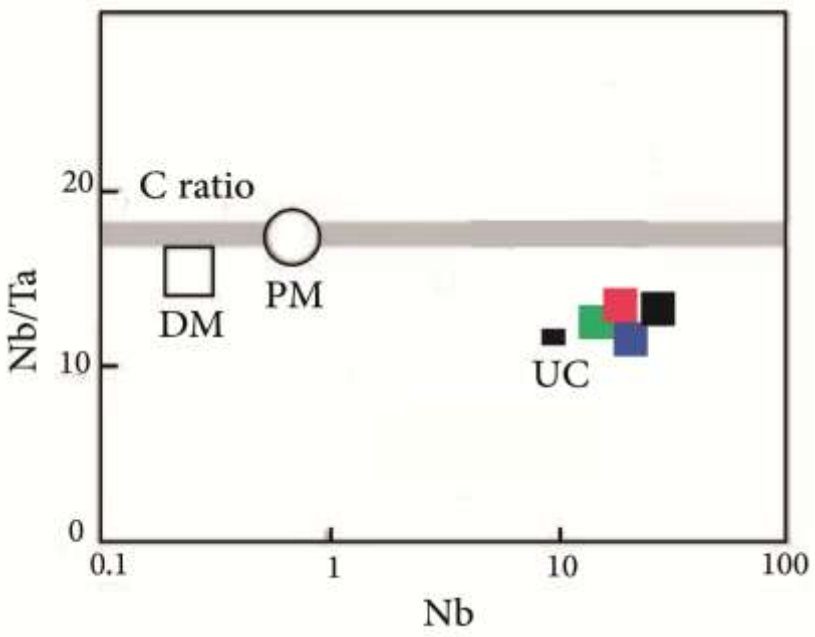

Figure 12 Nb vs. Nb/Ta plot to determine the origin of adakites where UC represents upper crustal adakites from (Wang et al, 2008). MORB representing the mid-ocean ridge was used from the data of (Niu and Batiza, 1997). (Symptoms are as in Figure 7 a)

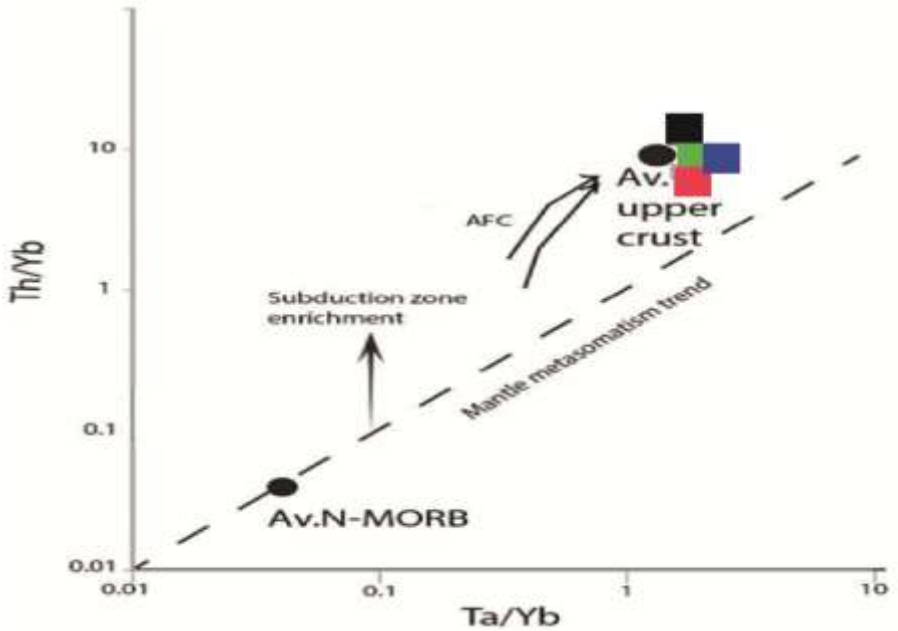

Figure 13 (Th/Yb) versus (Ta/Yb) diagram (Pearce, 1982) that the samples of the studied area have a composition very close to the average of the upper crust (signs like Figure 7 a).

 https://doi.org/10.5281/zenodo.14858968

ISSN: 0369-8963

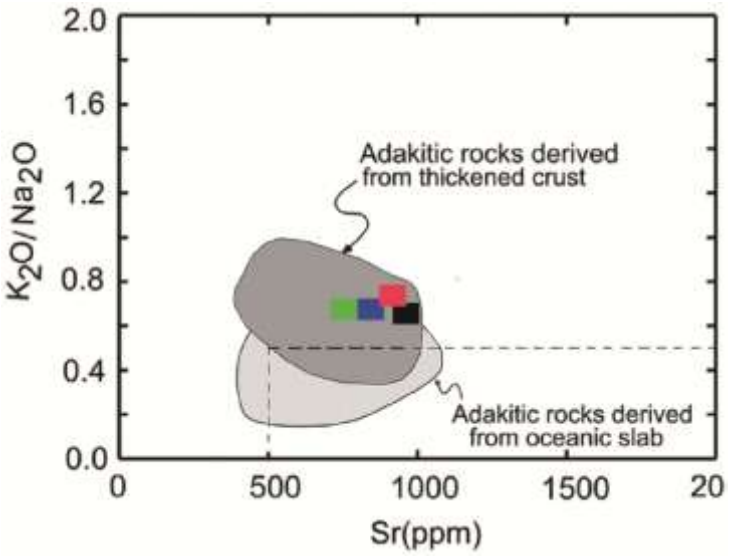

Figure 14 graph of Sr versus K_2O/Na_2O (Kamei et al., 2009: Eyuboglu et al., 2011). The origin of adakites in the studied area is from the melting of thick crust (symptoms are as in Figure 7 a).

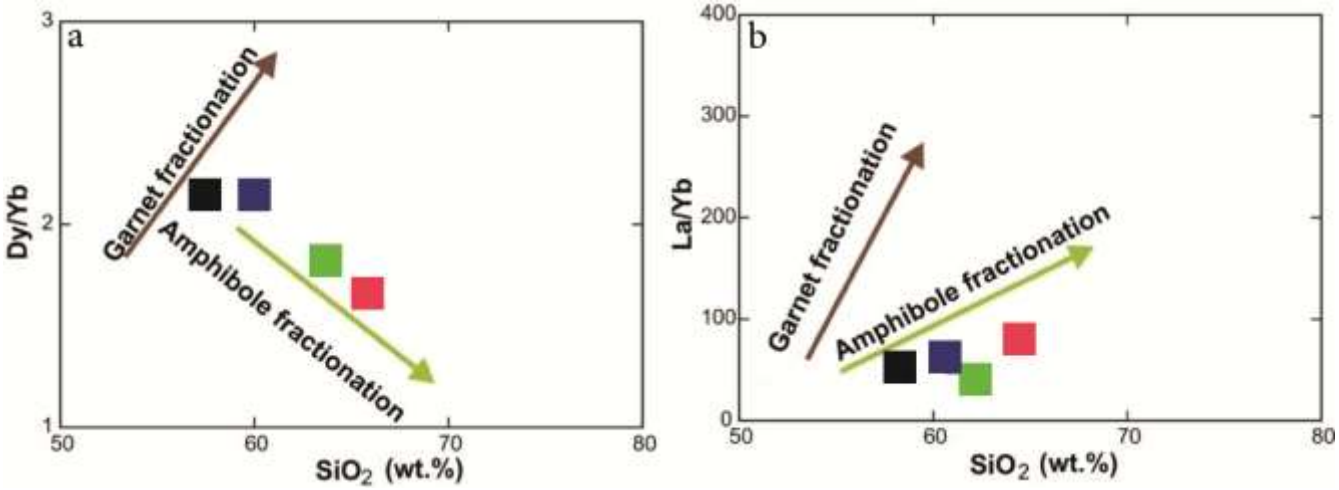

Figure 15 (a and b) Dy/Yb and La/Yb versus SiO_2 plot (Davidson et al, 2013), which shows that amphibole It is a main residual phase during melting in the samples of the studied area. (Symptoms are as in Figure 7 a).

The values of εNd(t) and Isr (initial ratios of $^{87}Sr/^{86}Sr$) related to the samples of the studied area are drawn in (Fig, 18) that the samples the studied area is located near the EMII range (Near the Upper Crust). It should be noted that EMI is related to the enriched mantle with moderate amounts of $^{87}Sr/^{86}Sr$, low amounts of $^{143}Nd/^{144}Nd$ and low ratios of $^{206}Pb/^{204}Pb$ and under the continental lithosphere Archean is placed with low values of Rb/Sr and Sm/Nd. While EMII is related to the enriched mantle with a high ratio of $^{87}Sr/^{86}Sr$, moderate values of $^{143}Nd/^{144}Nd$ and high ratios of $^{206}Pb/^{204}Pb$, which is in the subcontinental lithosphere from the Protozoic to the Phanerozoic (Zindler and Hart, 1986).

 https://doi.org/10.5281/zenodo.14858968

ISSN: 0369-8963

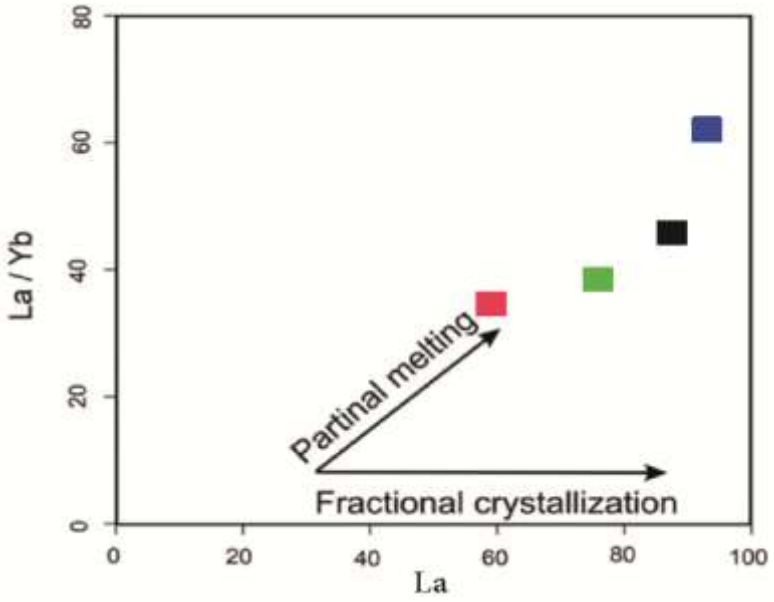

Figure 16 La/Yb vs. La graph (Gao et al, 2007), on which the samples of the studied area are marked and shows that more partial melting It is effective from recrystallization during the production of rocks in the studied area. (Symptoms are as in Figure 7 a).

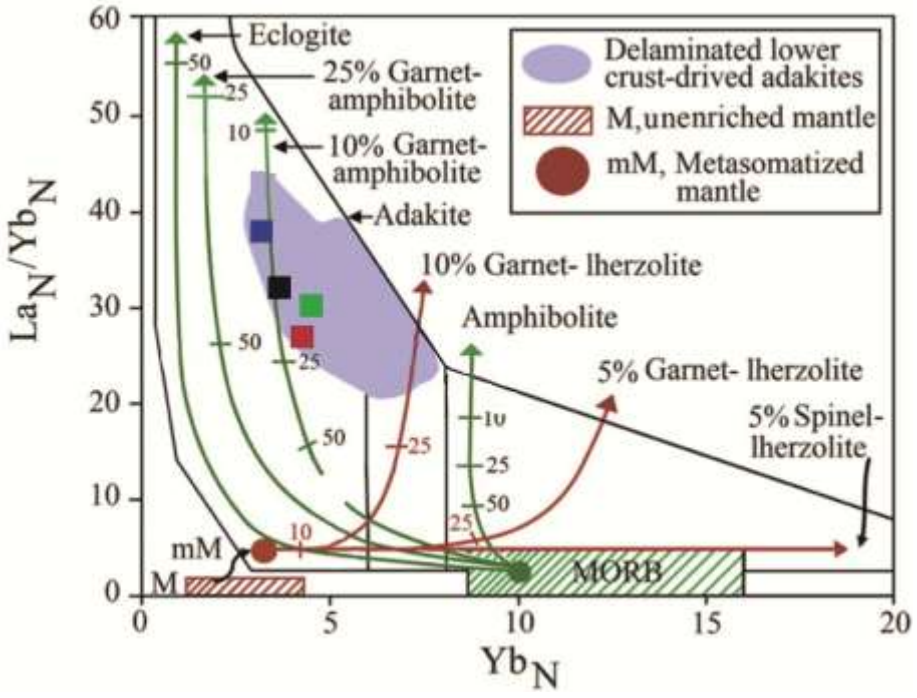

Figure17 LaN/YbN versus YbN diagram (Martin, 1986). Samples from the studied area could have been created by the melting of a 10% amphibolite garnet source. The region (delaminated lower rust-derived adakites) is from (Wang et al, 2006). The amounts of trace elements are from Sun & McDonough, 1989). (Symptoms are as in Figure 7 a).

 https://doi.org/10.5281/zenodo.14858968

Table 5: Analysis of the samples of the studied area by ICP-OES method in terms of (mg/kg) which were used to determine the grade and compare the distribution of elements (Ta: Trachy andesite, A: Andesite, D: Dacite)

Sample		Mi-5-1	mi-16	Mi-27	Mi-34
Longitude		48° 10'43.00"E	48° 4'33.40"E	48° 12'30.16"E	48° 2'43.60"E
Latitude		35°13'20.00"N	35°13'20.00"N	35° 17'32.61"N	35°12'28.00"N
Name		D	A	Ta	D
ppm	Al	1861.66	3185.25	81728.70	78863.23
	Ca	3745.70	5399.73	53473.86	25151.43
	Cr	-	888.75	-	-
	Fe	11638.01	12059.74	41021.34	28699.17
	Ge	-	-	51.60	-
	K	1667.17	18580.86	24176.04	17169.75
	Mg	827.35	532.68	7254.96	7054.70
	Mn	-	-	1379.77	-
	Na	2002.59	5752.37	18488.94	22587.59
	S	-	1172.08	2096.41	
	Sb	12844.87	9729.36	22830.78	25730.91
	Ti	-	486.24	4050.92	-

As can be seen in (Figure, 18), the samples of the studied area have been compared with BSE (bulk earth silicate) and mantle arrays. All the samples are located on the right side of the mantle array, where the so-called MORB-OIB-BSE trend (De Paolo and Wasserburg, 1979) and a negative correlation between the two parameters it shows the mentioned. Such correlation is generally attributed to magma interaction between crustal and mantle sources (e.g. Rollinson, 1993; Parada et al., 1999; Chen et al., 2002; Karsli et al. ., 2007, 2010). Experimental tests show that isotopic equilibrium is achieved faster than chemical equilibrium, and on the other hand, isotopic equilibrium in Sr element is achieved faster than Nd (Holden et al., 1987; Pin et al., 1990). By observing the data in (Table, 9), it is shown that the initial proportions of Sr in the samples of the studied area are more similar than the values of εNd. Therefore, the isotopic composition of Sr more than Nd has reached equilibrium. In the diagram of ($^{87}Sr/^{86}Sr$)t versus (εNdt), the samples of the studied area are located in the lower right quadrant (Fig, 19), in other words, the sample the studied area with low values of initial ratios of $^{87}Sr/^{86}Sr$ and low values of εNdt are placed in the enriched part compared to bulk earth compositions (Fig, 19).

 https://doi.org/10.5281/zenodo.14858968

ISSN: 0369-8963

Table 6 Chemical analyses for major and trace elements (Ta: Trachy andesite, A: Andesite, D: Dacite)

	Sample	mi-36 (Ta)	mi-34 (D)	mi-35 (A)	mi-31 (Ta)
	Longitude	48° 6'44.80"E	48° 2'43.60"E	48° 13'33.16"E	48° 12'37.04"E
	Latitude	35°11'58.20"N	35°12'28.00"N	35° 16'39.71"N	35° 17'15.95"N
Wt%	SiO_2	59.06	62.77	63.79	59.059
	TiO_2	0.68	0.69	0.48	0.68
	Al_2O_3	17.09	18.52	16.74	16.86
	Fe_2O_3(total)	5	4.25	4.82	5.72
	MnO	0.08	0.03	0.03	0.05
	MgO	2.50	0.28	1.29	1.49
	CaO	5.73	2.28	3.61	4.49
	Na2O	4.09	4.02	4.21	4.21
	K2O	2.79	2.74	3.09	2.87
	P2O5	0.31	0.31	0.23	0.29
	LOI	1.38	2.80	1.65	1.41
	Total	99.42	99.26	99.37	99.37
ppm	Li	10.2	3.17	12.9	16.2
	Be	3.16	3.37	2.98	2.67
	Sc	13.8	6.70	7.35	9.51
	V	109	78.7	65.9	80.4
	Cr	197	226	773	702
	Co	12.2	5.22	8.90	9.52
	Ni	15.3	9.06	23.9	22.8
	Cu	16.3	10.7	14.1	14.1
	Zn	70.6	57.9	52.8	59.2
	Ga	21.3	23.9	19.8	20.6
	Rb	85.3	91.6	100	95.6
	Sr	1214	865	1076	998
	Y	17.3	14.2	17.2	17.5

https://doi.org/10.5281/zenodo.14858968

Continued table 7

	Sample	mi-36 (Ta)	mi-34 (D)	mi-35 (A)	mi-31 (Ta)
ppm	Zr	202	302	185	181
	Nb	18.0	47.9	18.5	19.1
	Sn	2.22	2.16	2.25	1.97
	Cs	5.49	1.55	4.75	4.88
	Ba	1616	1542	1557	1591
	La	87.2	140	72.5	62.0
	Ce	148	270	120	107
	Pr	15.9	31.4	12.5	11.7
	Nd	52.1	109	39.1	39.0
	Sm	8.50	16.6	5.86	6.48
	Eu	2.03	4.17	1.56	1.79
	Gd	6.24	9.99	3.83	4.80
	Tb	0.91	1.16	0.56	0.69
	Dy	4.67	5.19	2.75	3.61
	Ho	0.88	0.86	0.52	0.66
	Er	2.43	2.16	1.45	1.79
	Tm	0.34	0.27	0.21	0.25
	Yb	1.68	1.56	1.95	1.90
	Lu	0.35	0.26	0.25	0.29
	Hf	5.29	6.83	4.85	4.83
	Ta	1.30	2.53	1.36	1.30
	Tl	0.38	0.24	0.33	0.54
	Pb	53.0	31.7	63.9	44.5
	Th	33.8	23.3	29.4	24.5
	U	9.05	4.62	7.12	7.53
	Sr/Y	70.17	123.33	62.55	57.02
	La/Yb	51.90	89.74	37.17	32.63

 https://doi.org/10.5281/zenodo.14858968

Table 8 Comparison of the samples of the studied area with the characteristics of adakites

Characteristics for adakites	Defantand Drummond(1990)	Martinetal (2005)	Azizi et al 2014 (B)*	Jahangiri 2007*	Case study			
					Mi-31	Mi-35	Mi-34	Mi-36
SiO_2	≥56wt%	>56wt%	>60wt%	65.4-73.2	59.06	62.77	63.79	62.13
Al_2O_3	≥15wt%	-	>15wt%	13.6-15.4	17.09	18.52	16.74	16.86
MgO	<3wt%	-	>2wt%	0.7-2.47	2.50	0.28	1.29	1.49
Y	≤18ppm	-	6.9-20.78	10-20	17.5	17.2	14.2	17.3
HREE	Low	-	Low	Low	Low	Low	Low	Low
Yb	≤1.9ppm	-	0.5-1.29	-	1.91	1.90	1.40	1.68
Sr	≥400ppm(rarely lower)	-	565-962	(346-737)	1214	865	1076	998
Sr/Y	≥ 40	-	>30	19.8-57.8	69.37	50.29	75.77	57.68
$^{87}Sr/^{86}Sr$	<.7040	-	0.7070-0.7079	-	0.7066	0.7064	0.7066	-
Na_2O	-	3.5-7.5wt%	3.82-4.82	2.75-5.21	4.09	4.02	4.21	4.21
K_2O/Na_2O	-	~0.42	0.74-1.02	>1	0.68	0.68	0.73	0.68
Mg#	-	~0.51(high)	0.12-0.55	0.37-0.62	0.62	0.62	0.66	0.55
La/Yb	-	>25	>20	-	45.65	41.73	51.78	36.90

Anyway, as discussed in the discussion of whole rock chemistry, it seems that the magmatic mixing process is one of the most important influencing processes in the geochemistry of the studied area. Here, the Sr and Nd isotopic ratios also confirm this. For example, magmas resulting from magmatic mixing show a curved arrangement (Figure 20) by plotting the primary isotope ratio of $^{87}Sr/^{86}Sr$ against Sr (Karsli et al., 2007). In addition, the image of isotopic ratios against silica can show the occurrence of reactions in the magma (Fig. 21 a and b) (e.g. Thiéblemont and Tegyey, 1994; Chen et al. al., 2002; Chen and Arakawa, 2005). In these graphs, there seems to be a strong relationship between ($^{87}Sr/^{86}Sr$) or εNdt and SiO_2 content (Figure 21 a and b). In the diagram ($^{87}Sr/^{86}Sr$) versus SiO_2 shows a amount of crustal contamination, which seems to indicate magmatic contamination as a dominant petrological process in combination with the effects of differential crystallization in it is effective during replacement of hybrid magma in the crust. The samples of the studied area are depicted in Nb/La, Ce/Pb, Ba/Nb and Th/Nb diagrams, which show that the high ratio of Ba/Nb and Th/ Nb has been introduced as crustal contamination (e.g. Thiéblemont and Tegyey, 1994; Chen et al., 2002; Chen and Arakawa, 2005), this also proves that crustal contamination It has been influential in the petrogenesis of samples from the informed area (Fig, 22 a-d). In general, by comparing the samples of the studied area with the neighboring areas, it can be said that the valuesof (εNd(t) and Isr (TDM) in the samples of the studied area with the isotopic values available in the studies (Azizi et al.,

 https://doi.org/10.5281/zenodo.14858968

2019) that were formed in the subduction environment show differences and are similar to studies (Azizi et al., 2014) that indicate the role of crustal materials in the origin of magma and at the same time, the collections in Turkey, whose origin is mainly mantle, have lower Isr values than the studied area (Fig, 23 a and b). According to Zartman and Doe (1980), the three reservoirs of upper mantle, lower crust, and upper crust can be distinguished based on their U, Th, and Pb concentrations. These elements are concentrated in the upper crust and the amount of U and Th is enriched compared to Pb. Meanwhile, the lower crust is depleted of Th and U, The upper mantle also has the amount of lead between the lower crust and the upper crust. Also, according to (Jackson and Dasgupta, 2008), enriched mantle 1 (EM1) has a low $^{206}Pb/^{204}Pb$ value, while enriched mantle 2 (EM2) It has an average value of $^{206}Pb/^{204}Pb$. Volcanic rocks studied in the charts of $^{206}Pb/^{204}Pb$ versus $^{207}Pb/^{204}Pb$ and $^{208}Pb/^{204}Pb$ above the line (NHRL) (North NHRL Hemisphere Reference Line) and between the mantle the top and the combination of the upper shell and (EM2) are placed (Fig. 24). Mineralogical evidence, however, Such as the sieve structures in plagioclase, does not allow the possibility of magma mixing to be completely discounted. The chemical compositions of the case study adakites do not match those of oceanic adakites (O-type: Defant and Drummond, 1990). But they are similar to type continental adakites (C-type: Castillo, 2006). O-type Adakites have a low ratio $^{87}Sr/^{86}Sr$ (<0.7040) and a high ratio $^{143}Nd/^{144}Nd$ (0.5128–0.5131), similar to MORB (Defant and Drummond, 1990). C-type adakites, which continental originate from the lower crust, generally Have diffrent the Sr and Nd isotope ratios: the C-type $^{87}Sr/^{86}Sr$ ratio ranges from 0.705 to 0.710, and $^{143}Nd/^{144}Nd$ ratio is much lower than that of O-type adakites (Defant et al., 1992; Kay et al., 1993; Stern and Kilian, 1996; Aguillón-Robles; et al., 2001). Plots of εtNd and $^{87}Sr/^{86}Sr$ (i) show that Case Study adakites are distinct from O-type adakites, they Have similarity to C-type adakites (Fig. 23 b). However, because of their relatively high $^{143}Nd/^{144}Nd$ and $^{87}Sr/^{86}Sr$ ratios, the Case Study adakites produced have been through the melting of continental crust at high pressure after the Arabian-Iranian collision. A number of different models there have been considered for origin. Some of these models include (1) melting of the oceanic in the eclogite and amphibolites facies (Defant and Drummond, 1990); (2) melting of the crust during or after continental collision (Arculus et al., 1999; Chung et al., 2003; Wang et al., 2007; Castillo, 2006, 2012); (3) fractional crystallization of mineral such as garnet from the basaltic arc parent magma during upwelling (Rodriguez et al., 2007); (4) derivation from primitive high-Mg andesite (Danyushevsky et al., the 2008). Adakite magma from oceanic slab has high silica content, meaning that much of it will crystallize when passing through the mantle; thus, the path adakite magma to the surface is not simple. Partial melting of metasomatic mantle with slab fluids, and which includes amphibole phlogopite, produces high-Mg andesite (Martin et al., 2005; Pallares et al., 2007; Danyushevsky et al., 2008; Castillo, 2008).The differentiation of minerals such as garnet and amphibole increases Sr/Y and La/Yb ratios to produce adakite magma (Castillo, 2012). (5) Finally, another possible origin of adakites high-Nb basalts. High-Nb basalts are characterized by high concentration of Nb(>20 ppm), HFSE, and alkali elements. The main Source of these rocks is partial melting slab of metasomatic mantle with slab melts of adakitic composition (Defant and Kepezhinskas, 2001; Leeman et al., 2005; Maury et al., 2009; Hastie et al., 2011).

 https://doi.org/10.5281/zenodo.14858968

ISSN: 0369-8963

Table 9 isotope analysis data of radiogenic elements Rb-Sr and Sm-Nd in the rocks of the study area based on the average age of 0.225 million years ago (based on figures 3 a and b).

Sample	Mi- 31	Mi- 34	Mi- 35
Age	0.225	0.225	0.225
SiO_2	59.059	63.7886	62.7662
Rb (ppm)	85.31739	100.4162	91.56632
Sr (ppm)	1214.423	1075.822	864.9494
$^{84}Sr/^{86}Sr$	0.05651	0.05652	0.05652
2s.e.	0.000011	0.000016	0.000020
$^{87}Sr/^{86}Sr$	0.706674	0.706659	0.706659
2s.e.	0.000011	0.000012	0.000014
^{85}Rb	0.000	0.000	0.000
^{88}Sr	11.225	9.400	7.645
$(^{87}Sr/^{86}Sr)i$	0.706673	0.706658	0.706488
ESr	_	_	_
Nd	52.08635	39.07883	46.81792
Sm	8.501686	5.862208	7.848176
$^{143}Nd/^{144}Nd$	0.512519	0.512532	0.512568
2 s.e	0.000004	0.000005	0.000004
$(^{143}Nd/^{144}Nd)i$	0.512519	0.512532	0.512568
EpsNdi	-2.32	-2.06	-1.36
$^{145}Nd/^{144}Nd$	0.348419	0.348419	0.348419
2 s.e	0.000003	0.000003	0.000003
^{142}Nd	9.99	7.70	8.78
^{147}Sm	0.002	0.001	0.001
$^{208}Pb/^{206}Pb$	2.0625	2.0647	2.0674
2 s.e	0.0000	0.0000	0.0000

https://doi.org/10.5281/zenodo.14858968

Continued table 9

Sample	Mi- 31	Mi- 34	Mi- 35
$^{207}Pb/^{206}Pb$	0.82816	0.83007	0.83247
2 s.e	0.00001	0.00001	0.00001
$^{208}Pb/^{204}Pb$	39.114	39.072	39.003
2 s.e	0.001	0.001	0.001
$^{207}Pb/^{204}Pb$	15.706	15.708	15.705
2 s.e	0.000	0.000	0.000
$^{206}Pb/^{204}Pb$	18.965	18.924	18.866
2 s.e	0.000	0.000	0.000
Pb Ion signal 208 strength(V)	21.7	17.0	21.1
Tl Ion signal strength(V) 205	3.5	3.5	3.4
TDM(Ga)	0.801	0.792	0.768
TDM.Gold	0.838	0.768	0.792
TDM.2stg	0.973	0.953	0.898

Azizi et al. (2013) believe in the northern SSZ, there are two rocks major groups of volcanic rocks that differ markedly in chemical composition and morphology: the first includes Intermediate to acidic rocks identified as adakite, and the second includes high-Nb basalts (HNB) that erupted in the Plio-Quaternary period. Azizi et al. (2013) demonstrated that the HNB were generated from partial melting of metasomatic mantle with adakitic melt. The two groups are closely related in space, and some fragments present of adakitic rocks are among the HNB. In general, by examining the models presented regarding the origin of adakites, it can be said that the adakites of the studied area are closer to model number 2 and were produced have been through the melting of continental crust at high pressure after the Arabian-Iranian collision.

 https://doi.org/10.5281/zenodo.14858968

ISSN: 0369-8963

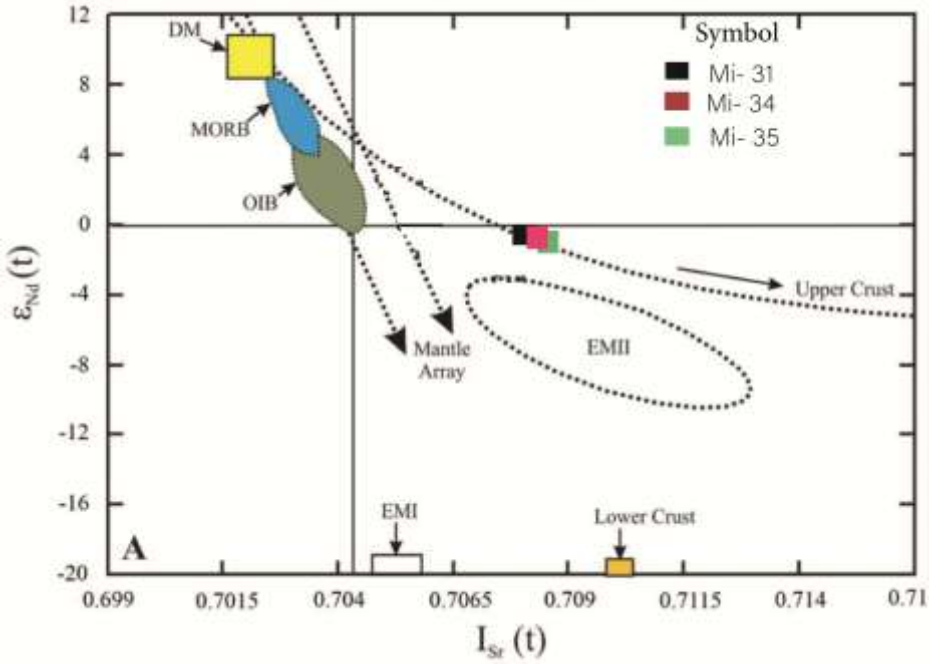

Figure18 The position of the studied samples in the graph of primary isotope ratios of $^{87}Sr/^{86}Sr$ against εNd(t), it can be seen in the graph that the values of εNd(t) and Isr in the samples related to the studied area are located near EMII according to the trend of placing the samples.

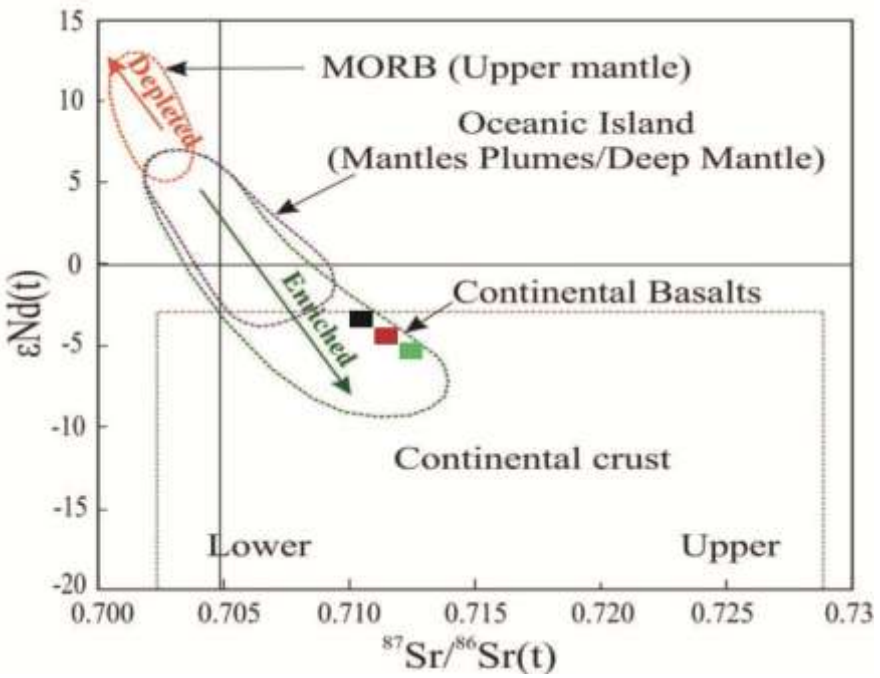

Figure 19 isotope ratio chart of t ($^{87}Sr/^{86}Sr$) against (εNdt) and the location of the samples of the study area that are in the enriched section compared to the bulk earth compounds. They take (Symptoms are similar to Figure 18).

https://doi.org/10.5281/zenodo.14858968

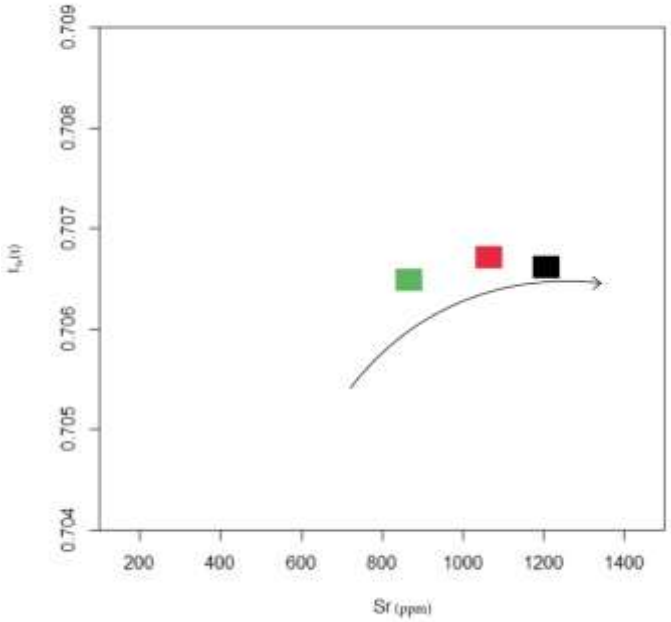

Figure 20: Curve arrangement, primary isotopic ratios of $^{87}Sr/^{86}Sr$ against Sr for the samples of the studied area (Karsli et al., 2007). (Symptoms are similar to Figure 19)

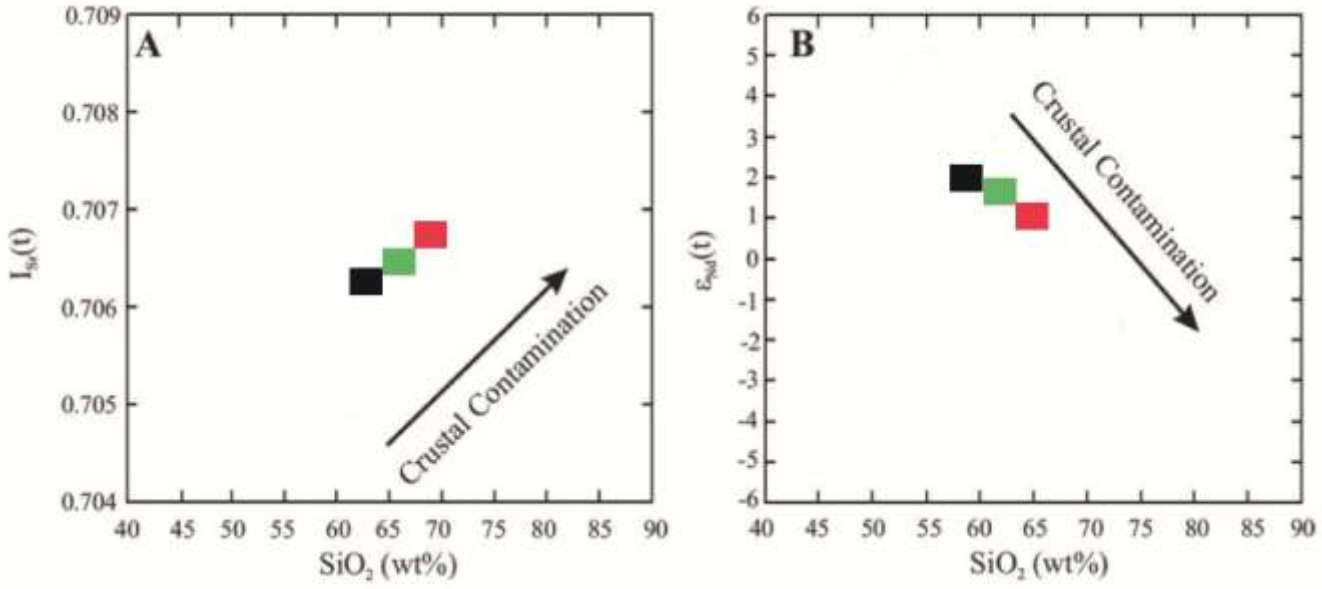

Figure 21 a and b) The increasing trend of primary isotopic ratios $^{87}Sr/^{86}Sr$ against SiO_2 indicates the role of magmatic contamination despite a strong relationship between ($^{87}Sr/ ^{86}Sr$) or ($\varepsilon Nd(t)$ and SiO_2 content. (Symbols are similar to Figure 19).

https://doi.org/10.5281/zenodo.14858968

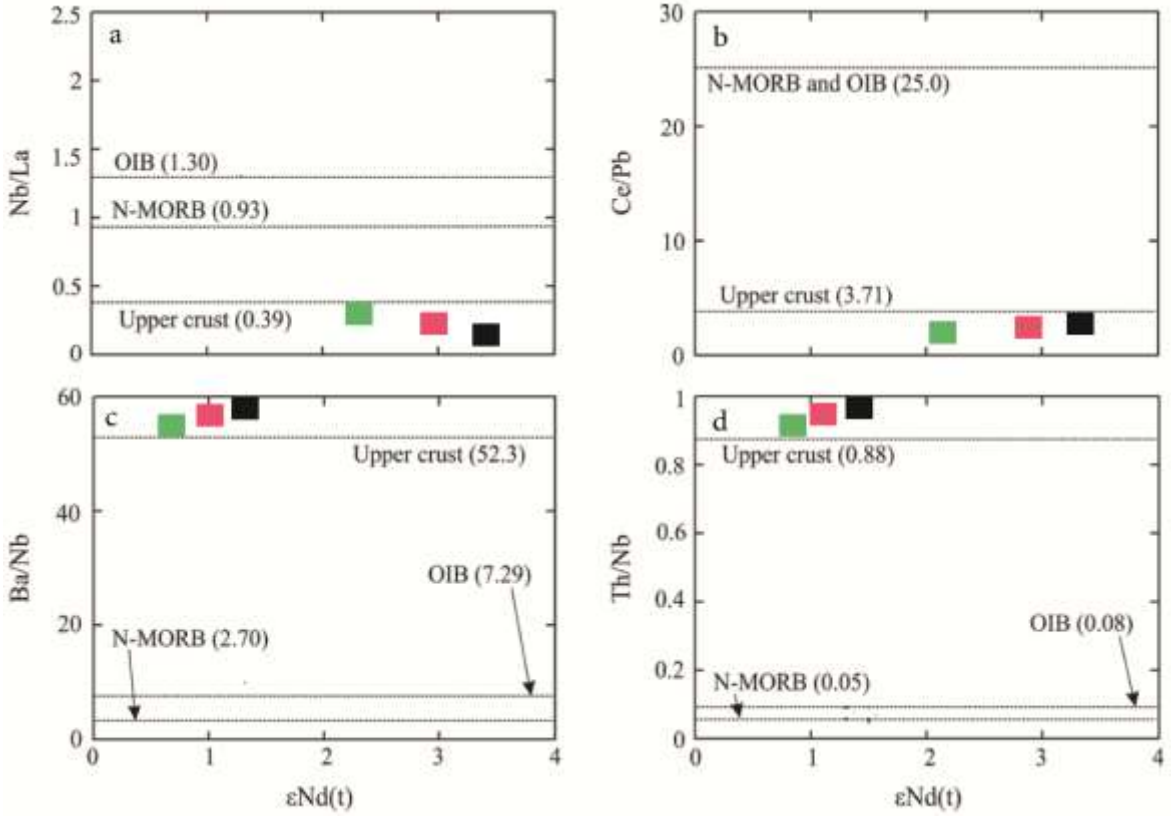

Figure 22 a-d) Binary graphs of the ratio of selected trace elements against (t) εNd for the samples of the studied area, which show the impact of crustal pollution in the petrogenesis of the samples The area is informed. The average values for OIB and MORB are from (after Sun and McDonough (1989) and the average value for the upper crust is from (after Rudnick and Gao (2003)). (Symbols are similar to It is Figure 19)

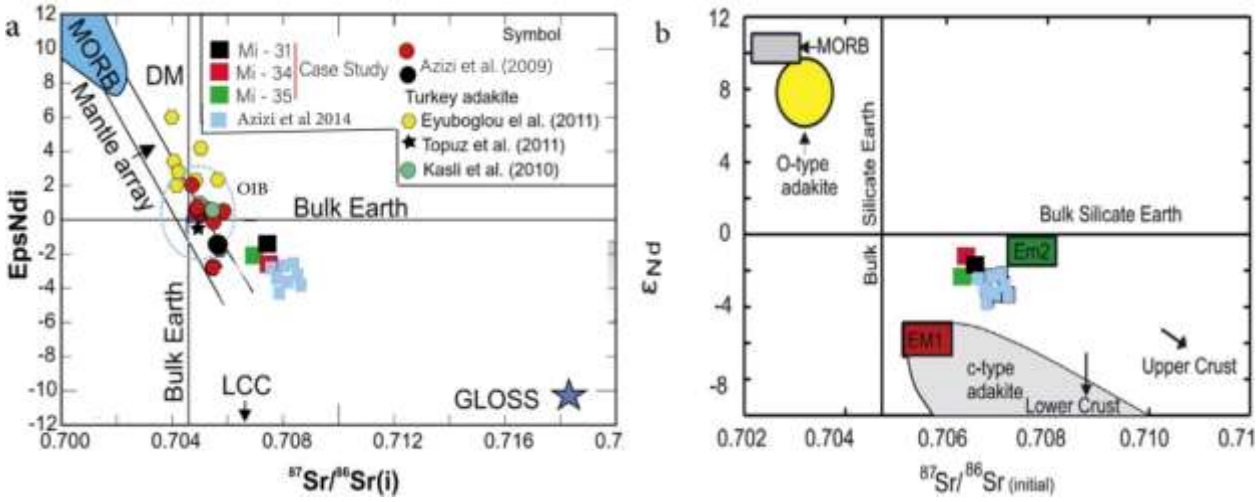

Figure 23 Comparison of the samples of the study area with the neighboring areas, a and b) difference in values of εNd(t) and Isr also (TDM) in the samples of the study area with the values The isotopes found in the studies (Azizi et al, 2019) that were formed in the subduction environment and the low Isr values of the Turkish complex with mainly mantle origin compared to the samples of the studied area and The similarity of the samples of the studied area with the studies (Azizi et al, 2014) which indicates the role of crustal materials in the origin of magma.

 https://doi.org/10.5281/zenodo.14858968

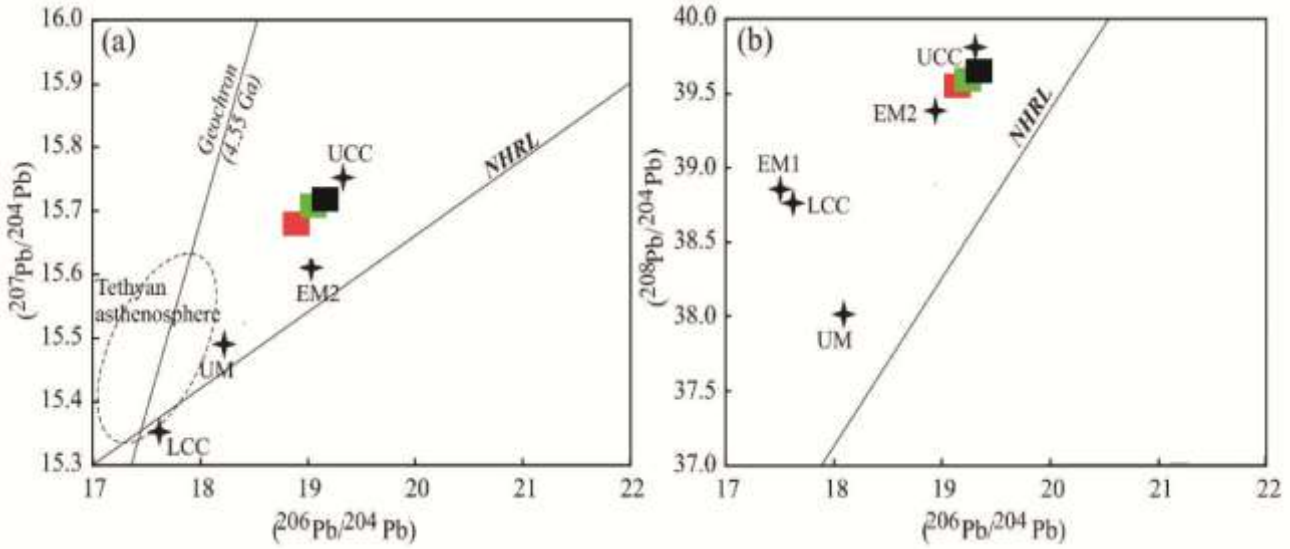

Figure 24 a and b) the location of the samples of the studied area on the isotope charts of $^{206}Pb/^{204}Pb$ versus $^{207}Pb/^{204}Pb$ and $^{208}Pb/^{204}Pb$. In these diagrams, samples are placed parallel to the NHRL trend and between the upper mantle and the upper crust (near the upper crust). The valuesof LCC, UCC and UM (Upper Mantle) are taken from (Zartman and Haines, 1988) and EM1 and EM2 from (Jackson and Dasgupta, 2008). (Symptoms are similar to Figure 19).

7. Conclusion

Quaternary volcanic adakites rocks in the west of Kohin, east of Qorveh (Northwest of Iran) In terms of rock group belonging to Trachy andesite, andesite, dacite. The studied samples have calc-alkaline nature. The calc-alkaline samples of the studied area are low-silica adakites and are closed to arc zones with the post-collision environment, and by determining their origin, it was found that the crust was the main responsible for the production of their productive magma. According to the Quaternary age of the samples in the study area, the rocks were formed after the continental collision between the Arabian plate and the Iranian platform, and definitely in post-collision conditions. The samples of the studied area are depicted in Nb/La, Ce/Pb, Ba/Nb and Th/Nb diagrams, which show that the high ratio of these elements has been introduced as crustal impurity isotope ratios confirm partial melting of the continental crust as sources of adakites in the case study. We therefore suggest melting of the crust after continental collision a partial source of adakites in this region based on the geochemistry of major, trace and rare earth elements and isotope ratios.

Acknowledgements: The authors are grateful to the research vicechancellor of the Tabriz University for assistance.

Funding: This research did not receive any specific grant from funding agencies in the public, commercial, or not-for profit sectors.

References

1. Agard, P., Omrani, J., Jolivet, L., Whitechurch, H., Vrielynck, man, W., B., Spak- Monié, P., Meyer, B., Wortel, R., 2011. Zagros orogeny: a subduction-dominated process. 148, 692–725, http://dx.doi.org/10.1017/S001675681100046X. Geological Magazine

2. Aguillón-Robles, A., Calmus, T., Benoit, M., Bellon, H., gois, Maury, R.C., Cotten, J., Bour J., chaud,F., 2001. Late Miocene adakite and Nb-enriched basalts from Vizcaino Peninsula, Mexico: indicators of East Pacific Rise subduction below southern Baja California. Geology 29, 531–534.

3. Ahmadzadeh, G; Jahangiri; A, David; Lentz M. (2010). Petrogenesis of Plio-Quaternary post-collisional ultrapotassic volcanism in NW of Marand, NW Iran. , 39(1-2), 0–50. doi:10.1016/j.jseaes.2010.02.008

4. Arculus, R.J., Lapierre, H., Jaillard, E., and 1999. Geochemical window into subduction accretion processes: raspas metamorphic 547–550. complex, Ecuador. Geology 27.

5. Atherton, M., Petford, N., 1993. Generation of sodium-rich magmas from newly underplated http://dx.doi.org/10.1038/362144a0. basaltic crust. Nature 362, 144–146.

6. Azizi, H., Asahara, Y., 2013. Juvenile granite in the Late Jurassic–Early Sanandaj-Sirjan zone, NW Iran: Cretaceous arc-continent collision. International Geology Review 55, 1523–1540.

7. Azizi, H., Asahara, Y., Tsuboi, M., Takemura, K., & Razyani, S. (2014). The role of heterogenetic mantle in the genesis of adakites northeast of Sanandaj, northwestern Iran. Geochemistry, 74(1), 87-97.

8. Azizi, H., Jahangiri, A., 2008, Cretaceous subduction-related volcanism in the northern Sanandaj-Sirjan Zone, Iran: Journal of Geodynamics, v. 45, p. 178–190.

9. Azizi, H., Moinevaziri, H., 2009. Review of the tectonic setting of Cretaceous to quaternary volcanism in northwestern Iran. Journal of Geodynamics 47, 167–179.

10. Azizi, H., Stern, R. J., Topuz, G., Asahara, Y., & Moghadam, H. S. (2019). Late Paleocene adakitic granitoid from NW Iran and comparison with adakites in the NE Turkey: Adakitic melt generation in normal continental crust. Lithos, 346, 105151.

11. Berberian, M. and King, G.C.P., 1981. Towards a paleogeography and tectonic evolution of Iran. Canadian journal of earth sciences 18: 210-265.

12. Boccaletti, M., Innocenti, F., Manetti, P., Mazzuoli, T., Motamed, A., Pasquare, G., Radicati di Brozolo, F., Amin Sobhani, E., 1976. Neogene and Quaternary volcanism of the Bijar area (Western Iran). Bulletin of Volcanology 40, 121–132.

13. Castillo, P.R., 2012. Adakite petrogenesis. Lithos 134–135, 304–316.

14. Castillo, P.R., 2006. An overview of 51, adakite petrogenesis. Chinese Science Bulletin 257–268.

15. Castillo, P.R., Janney, P.E., Solidum, R., 1999. Petrology and geochemistry of Camiguin Island, southern Philippines: insights into the source of adakite and other lavas in a complex arc tectonic setting. Contributions to Mineralogy and Petrology 134, 33–51.

16. Castillo, P.R., 2008. Origin of the adakite–high-Nb cations basalt association and its imply for post subduction magmatism Society in Baja California, Mexico. Geological of America Bulletin 120, 451–462.

17. Chang, S.J., Marone, F., Romanowicz, Pasyanos, B., van der Lee, S., Matzel, E.M., Flanagan, M.P., M., Schmid, C., Bedle, dimensional H., Rodgers, A.J., 2010. Joint inversion for three- S velocity mantle Geophysical structure along the Tethyan margin. Journal of Research 115, http://dx.doi.org/10.1029/2009JB007204.

18. Chen; B. Arakawa Y. (2005). Elemental and Nd-Sr isotopic geochemistry of granitoids from the West Junggar foldbelt (NW China), with implications for Phanerozoic continental growth. , 69(5), 0–1320. doi:10.1016/j.gca.2004.09.019

19. Chen, B., Jahn, B.M., Wei, C. (2002) Petrogenesis of Mesozoic granitoids in the Dabie UHP complex, Central China: trace element and Nd–Sr isotope evidence. Lithos 60, 67–88.

20. Chiaradia, M., 2009. Adakite-like melting-assimilation magmas from fractional crystallization and of mafic Cordillera, lower crust (Eocene Macuchi arc, Western Ecuador). Chemical Geology 265, 468–487.

21. Chung, S. L., Liu, D.Y., Ji, J. Q., Chu, M. F., Lee, H.Y.,Wen, D. J., Lo, C. H., Lee, T.Y.,Qian, Q. & Zhang, Q. (2003). Adakites from continental collision zones: melting of thickened lower crust beneath southernTibet. Geology 31, 1021-1024.

22. Dabiri, R., Emami, M., Mollaei, H., Chen, B., Abedini, M., Om-ran, N., & Ghaffari, M. (2011). Quaternary postcollision alkalinevolcanism NW of Ahar (NW Iran): Geochemical constraints offractional crystallization process. Geologica Carpathica, 62(6),547– 562.

23. Danyushevsky, L.V., Falloon, T.J., Crawford, A., A.J., Tetroeva, S.A., Leslie, R.L., Verbeeten, 2008. High-Mg adakites from evidence Kadavu Island Group, Fiji, southwest Pacific: for the mantle origin http://dx.doi.org/10.1130/G24349A.1. of adakite parental melts. Geology 36, 499–502.

24. Davidson, J., Turner, S., Plank, T., 2013. Dy/Dy*: variations arising from mantle sources and petrogenetic processes. Journal of Petrology 54, 525–537.

25. Defant, M.J., Drummond, M.S., magmas 1990. Derivation of some modern arc by melting Of young subducted lithosphere. Nature 347, 662–665.

26. Defant, M.J., Jackson, T.E., Drummond, M.S., de Boer, J.Z., Bellon, H., Feigenson M.D., Maury, R.C., Stewart, R.H., 1992. The geochemistry of young volcanism throughout western Panama and southeastern Costa Rica: an overview. Journal of the Geological Society 149, 569–579.

27. Defant, M.J., Kepezhinskas, P., 2001. EOS Evidence suggests slab melting in arc magmas. 82, 62–69.

28. Defant, M.J., Richerson, P.M., De Boer, Drummond, J.Z., Stewart, R.H., Maury, R.C.,Bellon, H., M.S., Feigenson, M.D., slab melting Jackson, T.E., 1991. Dacite genesis viaBoth and differentiation: Panama. Petrogenesis of La Yeguada Volcanic Complex, Journal Of Petrology 32, 1101–1142.

29. Defant, M.J., Xu, J.F., Kepezhinskas, P., Wang, Q., Zhang, Q., Xiao, L., 2002. Adakites: some variations on a theme. Acta Petrologica Sinica 18, 129–142.Ding, L., Kapp, P., Yue, Y., Lai, Q., 2007. Postcollisional calc-alkaline lavas and xenoliths from the Southern Qiangtang terrane, central Tibet. Earth and Planetary Science Letters 254, 28– 38.

30. DePaolo, D.J., Wasserburg, G.J., 1976. Geophysical Nd isotopic variations and petrogenetic models. Research Letters 3, 249–252.

31. Eyuboglu, Y., Santosh, M., Chung, S.L., mas 2011. Crystal fractionation of adakitic mag-in the crust–mantle transition zircon zone: petrology, geochemistry and U–Pb chronology of the Seme adakites, eastern, Pontides, NE Turkey. Lithos 121, 151–166.

32. Faridazad, M. (2020). Petrology, geochemistry, and petrogenesis of two-pyroxene andesites in the northwest of Varzaghan (NW Iran): An evidence of calc-alkaline magmatism in a post-collisional setting. Iranian Journal of Petrology, 11, 37– 64 (in Persian with English abstract) https://doi.org/10.22108/ijp.2020.113825.1102.

33. Gao, S., Rudnick, R.L., Yuan, H.L., Liu, X.M., Xu, W.L., Lin, W.L., Ayers, J., Wang,cX.C. and Wang, Q.H., 2004. Recycling lower continental crust in the North ChinacCraton. Nature 432: 892–897.

34. Gao, Y., Hou, Z., Kamber, B. S., Wei, R., Meng, X., & Zhao, R. (2007). Adakite-like porphyries from the southern Tibetan continental collision zones: evidence for slab melt metasomatism. Contributions to Mineralogy and Petrology, 153, 105-120

35. Ghasemi, A., Talbot, C.J., 2006. A new (Iran). Tectonic scenario for the Sanandaj-Sirjan Zone Journal of Asian Earth Sciences 26, 683–693.

36. Ghorbani, M.R., Bezanjani, R.N., 2011. Tizing Slab partial melts from the metasoma- agent to adakite, Tafresh Eocene volcanic rocks, Iran. Island Arc 20, 188–202.

37. Goss, A.R., Kay, S.M., 2009. Extreme high field strength element (HFSE) depletion and near-chondritic Nb/Ta ratios in Central Andean adakite-like lavas (28oS, 68oW). Earth and Planetary Science Letters 279, 97–109.

38. Guan, Q., Zhu, D.C., Zhao, Z.D., Zhang, L.L., Liu, M., Li, X. W, Yu, F., Liu, M. H. and Mo, X. X., 2010. Late Cretaceous adakites from the eastern segment of the Gangdese Belt, Southern Tibet: prod-ucts of Neo-Tethyan mid-ocean ridge subduction. Acta Petrologica Sinica 26: 2165–2179 (in Chinese with English abstract).

39. Haschke, M., Siebel, W., Günther, A., Scheuber, E., 2002. Repeated crustal thickening and recycling during the Andean orogeny in north Chile (21°–26°S). J. Geophys. Res.Solid Earth 107 (ECV 6–1–ECV 6–18).

40. Haschke, M., & Gunther, A. (2003). Balancing crustal thickening in arcs by tectonic vs. magmatic means. Geology, 31(11), 933-936.

41. Hastie, A. R., Mitchell, S. F., Kerr, A. C., Minifie, M. J., & Millar, I. L. (2011). Geochemistry of rare high-Nb basalt lavas: Are they derived from a mantle wedge metasomatised by slab melts?. Geochimica et Cosmochimica Acta, 75(17), 5049-5072.

42. Holden, P., Halliday, A.N., Stephens, W.E. (1987) Neodymium and strontium isotope content of microdiorite enclaves points to mantle input to granitoid production. Nature 330, 53–56.

43. Hou, Z.Q., Gao, Y.F., Qu, X.M., Rui, Z.Y., generated Moc, X.X., 2004. Origin of adakitic intrusive during mid-Miocene and Planetary east–west extension in southern Tibet. Earth Science Letters 220, 139–155.

44. Jackson, M. G., & Dasgupta, R. (2008). Compositions of HIMU, EM1, and EM2 from global trends between radiogenic isotopes and major elements in ocean island basalts. Earth and Planetary Science Letters, 276(1-2), 175-186.

45. Jahangiri, A. (2007). Post-collisional Miocene adakitic volcanism in NW Iran: Geochemical and geodynamic implication. Journal of Asian Earth Sciences, 30(3-4), 433 – 447. https://doi. org/10.1016/j.jseaes.2006.1

46. Kalfoun, F., Ionov, D., Merlet, C., 2002. matised, HFSE residence and Nb/Ta ratios in metaso- rutile-bearing mantle peridotites. Earth and Planetary Science Letters 199,49–65.

47. Kamei, A., Miyake, Y., Owada, M., Kimura, partial J.I., 2009. A pseudo adakite derived from melting of tonalitic to granodioritic Lithos crust, Kyushu, southwest Japan arc. 112, 615–625.

48. Kamvong, T., Zaw, K., Meffre, S., Maas, R., Stein, H., Lai, Ch. K., 2014. Adakites intheTruong Son and Loei fold belts, Thailand and Laos: genesis and implications for geodynamics and metallogeny. Gondwana Research 26: 165–184.

49. Karsli, O., Chen, B., Aydin, F., Sen, C. (2007) Geochemical and Sr–Nd–Pb isotopic compositions of the Eocene Dölek andSariçiçek Plutons, Eastern Turkey: implications for magma interaction in the genesis of high-K calc-alkaline granitoids in apost-collision extensional setting. Lithos 98, 67–96.

50. Karsli, O., Dokuz, A., Kandemir, R., Aydin, F., Schmitt, A. K., Ersoy, E. Y., & Alyıldız, C. (2019). Adakite-like parental melt generation by partial fusion of juvenile lower crust, Sakarya Zone, NE Turkey: a far-field response to break-off of the southern Neotethyan oceanic lithosphere. Lithos, 338, 58-72.

51. Karsli, O., Dokuz, A., Uysal, ˙I., Aydın, of F., Kandemir, R., Wijbrans, R.J., 2010. Generation the early Cenozoic adakitic volcanism Eastern by partial melting of mafic lower crust, Turkey: implications for Crustal thickening to delamination. Lithos 114, 109–120.

52. Kay, R.W., 1978. Aleutian magnesian andesites: melts from subducted Pacific Ocean crust. Journal of Volcanology and Geothermal Research 4: 117–132.

53. Kay, R.W., Kay, S.M., 2002. Andean adakites: three ways to make them. Acta Petrologica Sinica 18, 303–311.

54. Kay, S. Mahlburg, Mpodozis, C.. Ramos. V.A. and Munizaga, F., 1991. Magma source regions for mid to late Tertiary volcanic rocks and erupted over a shallowing subduction zone and through a thickening crust in the main Andean Cordillera (28-33”s). In: R.S. Harmon and C.W. Rapela (Editors), Andean Magmatism and its Tectonic Setting. Geol. Sot. Am., Spec., Pap., 265: 113-137.

55. Kay, S.M., Mpodozis, C., and Coira, B., 1999. Neogene magmatism, tectonism, and mineral deposits of the Central Andes (22° to 33°S latitude), in Skinner, B.J., ed., Geology and ore deposits of the Central Andes: Society of Economic Geologists, Special Publication 7, 27– 59.

56. Kay, S.M., Ramos, V.A., Marquez, M., of 1993. Evidence in Cerro Pampa volcanic rocks Slab melting prior to ridge trench collision in southern South America. Journal of Geology 101, 703–714.

57. Khan Nazer, N.H., Jalali, A., Saidi, A., Helmi, F. Mohtat, F., Bahreh, M., Geological Map Of Kuhin, 1:100000 Series, Sheet No. 5660

58. Kolb M, A., Quadt V, Peytcheva I, Heinrich C A, Fowler S J and Cvetkovic V (2003) 4 Adakite-like and Normal Arc Magmas: Distinct Fractionation Paths in the East Serbian.

59. Küster, D., & Harms, U. (1998). Post-collisional potassic granitoids from the southern and northwestern parts of the Late Neoproterozoic East African Orogen: a review. Lithos, 45(1-4), 177-195.

60. Leake, B.E., et al. (1997) Nomenclature of Amphiboles: Report of the Subcommittee of the International Mineralogical Association, Commission on New Minerals and Mineral Names. American Mineralogist, 82, 1019-1037.http://dx.doi.org/10.1180/minmag.1997.061.405.13

61. LeBas, M.J., LeMaitre, R.W., Streckeisen, A., Zanettin, B., 1986. A chemical classification of volcanic rocks based on the total alkali silica diagram. Journal of Petrology 27, 745–750.

62. Lechmann, A., Burg, J. P., Ulmer, P., Guillong, M., & Faridi, M. (2018). Metasomatized mantle as the source of Mid-Miocene- Quaternary volcanism in NW-Iranian Azerbaijan: Geochrono logical and geochemical evidence. Lithos, 304-307, 311– 328.

63. Leeman, W.P., Lewis, J.F., Evarts, R.C., Conrey, R.M., Streck, M.J., constraints 2005. Petrologic on the thermal structure of the Cascades arc. Journal of Volcanology and Geothermal Resource 140, 67–105.

64. Li. Xiao; J.D. Clemens (2007). Origin of potassic (C-type) adakite magmas: Experimental and field constraints. , 95(3-4), 399–414. doi:10.1016/j.lithos.2006.09.002 .

65. Ma, C., Li, Z., Ehlers, C., Yang, K., Wang, R., 1998. A post-collisional magmatic plumbing system: Mesozoic granitiod plutons from the Dabie high-pressure and ultrahighpressure metamorphic zone, east-central China. Lithos 45, 431–457.

66. Malecootyan, S., Hagh-Nazar, S.H., Ghorbani, M., Emami, M.H., 2007. Magmatic evolution in quaternary basaltic rocks in Sanandaj–Takab axis. Geosciences Sci- entific Quarterly Journal (Geological Survey of Iran) 64, 166–178 (in Persian with English abstract).

67. Maniar, P. D., & Piccoli, P. M. (1989). Tectonic discrimination of granitoids. Geological society of America bulletin, 101(5), 635-643.

68. Mansouri Esfahani, M., Khalili, M., Kochhar, N., and Gupta, L.N., 2010, A-type granite of the Hasan Robat area (NW of Isfahan, Iran) and its tectonic significance: Journal of Asian Earth Sciences, v. 37, p. 207–218.

69. Martin, H., 1986. Effect of steeper Archean geothermal gradient on geochemistry of subduction-zone magmas. Geology 14, 753–756.

70. Martin, H., Smithies, R.H., Rapp, R.P., Moyen, J-F. and Champion, D.C., 2005. An overview of adakite, tonalite–trondhjemite–granodiorite (TTG) and sanukitoid: relationships and some implications for crustal evolution. Lithos 79 (1–2): 1–24.

 https://doi.org/10.5281/zenodo.14858968

71. Martin, H. (1999). The adakitic magmas: Modern analogues of Archean granitoids. Lithos, 46(3), 411– 429. https://doi.org/10.1016/S0024- 37(98)00076-0.

72. Martınez- Serrano, R.G., Schaaf, P., Solıs-Pichardo, G., Hernandez-Bernal, M., Hernandez- Trevino, T., Morales-Contreras, J.J., Luis Macıas, J., 2004. Sr, Nd and Pb isotope and geochemical data from the Quaternary Nevado de Toluca volcano, a source of recent adakitic magmatism, and the Tenango Volcanic Field, Mexico. Journal of Volcanology and Geothermal Research 138, 77–110.

73. Maury, R., Calmus, T., Pallares, C., Benoit, M., Grégoire, M., Aguillón-Robles, A., Bellon, H., Bohn, M., 2009. Origin of the adakite–high-Nb basalt association and its implications for postsubduction magmatism in Baja California. Mexico: Discussion. GSA Bulletin 121, 1465–1469, http://dx.doi.org/10.1130/B30043.1.8. Omrani et al., 2008 Pang et al. (2016)

74. Morimoto, N. (1989). Nomenclature of pyroxenes. Mineralogical Journal, 14(5), 198-221.

75. Morris, J.D., 1995. Slab melting as an explanation of Quaternary volcanism and aseismicity in southwestern Japan. Geology 23, 395–398.

76. Niu, Y., & Batiza, R. (1997). Trace element evidence from seamounts for recycled oceanic crust in the Eastern Pacific mantle. Earth and Planetary Science Letters, 148(3-4), 471-483.

77. Okay, A.I., Altherr, R., Schwarz, W.H., Siebel, W., Zack, T., Satır, M., S¸ en, C., 2011. Post-collisional adakite-like magmatism in the A gvanis Massif and implications for the evolution of the Eocene magmatism in the Eastern Pontides (NE Turkey). Lithos 125, 131–150.

78. Omrani, J., Agard, P., Whitechurch, H., Benoit, M., Prouteau, G., & Jolivet, L. (2008). Arc-magmatism and subduction history beneath the Zagros Mountains, Iran: A new report of adakites and geodynamic consequences. Lithos, 106(3-4), 380 – 398. https://doi.org/10.1016/j.lithos.2008.09.008.

79. Pallares, C., Maury, R.C., Bellon, H., Royer, J.-Y., Calmus, T., Aguillón Robles, A., Cotton, J., Benoit, M., Michard, F., Bourgois, J., 2007. Slab-tearing following ridge-trench collision: California, evidence from Miocene volcanism in Baja Mexico. Journal of Volcanology and Geothermal Research 161, 95–117.

80. Pang, K. N., Chung, S. L., Zarrinkoub, M. H., Li, X. H., Lee, H. Y., Lin, T. H., & Chiu, H. Y. (2016). New age and geochemical constraints on the origin of Quaternary adakite-like lavas in the Arabia-Eurasia collision zone. Lithos, 264, 348 – 359. https://doi. org/10.1016/j.lithos.2016.08.042.

81. Parada, M.A., Nyström, J.O., Levi, B. (1999) Multiple sources for the Coastal Batholith of central Chile (31-34°S): geochemical and Sr-Nd isotopic evidence and tectonic implications. Lithos, Vol. 46, p. 505–521.

82. Pearce, J. A. (1996). A user's guide to basalt discrimination diagrams. Trace element geochemistry of volcanic rocks: applications for massive sulphide exploration. Geological Association of Canada, Short Course Notes, 12, 79-113.

83. Pearce, J. A. (1982). Trace element characteristics of lavas from destructive plate boundaries. Orogenic andesites and related rocks, 528-548.

84. Peccerillo, A., Taylor, T.S., 1976. Geochemistry of Eocene calc alkaline volcanic rocks from Kastamonu area, northern Turkey. Contributions to Mineralogy and Petrology 58, 63–81.

85. Pin, C., 1990. Evolution of the lower crust in the Ivrea zone: a model based on isotopic and geochemical data. Granulites and crustal evolution. Springer, Netherlands, pp. 87–110.

86. Prouteau, G., Scaillet, B., Pichavant, M., & Maury, R. (2001). Evidence for mantle metasomatism by hydrous silicic melts derived https://doi.org/10.1038/35065583

87. Q. Qian, J. Hermann (2013). Partial melting of lower crust at 10–15 kbar: constraints on adakite and TTG formation, Published in Contributions to Mineralogy and Petrology, 165(6), 1195–1224. doi:10.1007/s00410-013-0854-9,

88. Rapp, R.P., Watson, E.B., Miller, C.F., 1991. Partial melting of amphibolite/eclogite and the origin of Archaean trondhjemites and tonalites. Precambrian Research 51, 1–25.

89. Richards, J.P., Wilkinson, D., Ullrich, T., 2006. Geology of the Sari Gunay epithermal golddeposit, northwest Iran. Economic Geology 101, 1455–1496.

90. Rickwood, P. C. (1989). Boundary lines within petrologic diagrams which use oxides of major and minor elements. lithos, 22(4), 247-263.

91. Rodriguez, C., Selles, D., Dungan, M., Langmuir, C., Leeman, W., 2007. Adakitic dacites formed by intracrustal crystal fractionation of water-rich parent Nevado magmas at de Longav volcano (36.2 degrees S; Andean Southern Volcanic Zone, central Chile). Journal of Petrology 48, 2033–2061.

92. Rollinson, H.R., 1993. Using Geochemical Data: Evaluation, Presentation, Interpretation. Longmans, Harlow, 325 pp.

93. Rudnick, R.L. and Gao, S., 2003. composition of the continental crust. In: Holland, H.D., Turekian, K.K. (Eds.). Treatise on Geochemistry 3: 1–64.

94. Saunders, A. D., Tarney, J., & Weaver, S. D. (1980). Transverse geochemical variations across the Antarctic Peninsula: implications for the genesis of calc-alkaline magmas. Earth and Planetary Science Letters, 46(3), 344-360.

95. Segment of the Balkan-Carpathian Arc. Journal of petrology 54 (3): 421-451.

96. Şengör and Kidd, 1979 Schmidt, M.W., Dardon, A., Chazot, G., Vannucci, R., 2004. The dependence of Nb and Ta rutile–melt partitioning on melt composition and Nb/Ta fractionation during subduction processes. 4 earth and planetary science letters 226, 15–432.

97. Sepahi, A.A., Athari, S.F., 2006. Petrology of major granitic plutons of the northwestern part of the Sanandaj–Sirjan Metamorphic Belt, Zagros Orogen, Iran: with emphasis on A-type granitoids from the SE Saqqez area. Neues Jahrbuch für Mineralogical Abh 93–106 183/1

98. Shahbazi, H., Siebel, W., Pourmoafee, M., Ghorbani, M., Sepahi, A.A., Shang, C.K., and Vousoughi Abedini, M., 2010, Geochemistry and U–Pb zircon geochronology ofthe Alvand plutonic complex in Sanandaj-Sirjan Zone (Iran): New evidence for Jurassic magmatism: Journal of Asian EarthSciences, v. 6, p. 668–683.

99. Stern, C.R., Kilian, R., 1996. Role of the subducted slab, mantle wedge and continental crust in the generation of adakites from the Austral Volcanic Zone. Contributions to Mineralogy and Petrology 123, 263–281.

100. Stocklin, J., Nabavi, M., 1972. Tectonic Map of Geological Survey of Iran.

101. Sun, S.S., McDonough, W.F., 1989. Chemical and isotopic systematic of ocean basalts: implications for mantle composition and process. In: Saunders, A.D., Norry, M.J. (Eds.), Magmatism in Ocean Basins. Geological Society, Special Publications 42, London, pp. 313–345.Thirlwall and Jones, Iran.Topuz, G., 1993

102. Thiéblemont, D., & Tegyey, M. (1994). Une discrimination géochimique des roches différenciées témoin de la diversité d'origine et de situation tectonique des magmas calco-alcalins. Comptes rendus de l'Académie des sciences. Série 2. Sciences de la terre et des planètes, 319(1), 87-94.

103. Topuz G., Okay A. I., Altherr R. et al. 2011. Post-collisional adakite-like magmatism in the Agvanis Massif and implications for the evolution of the Eocene magmatism in the Eastern Pontides (NE Turkey). Lithos 125, 131–150

 https://doi.org/10.5281/zenodo.14858968

104. Varol, E., Temel, A., Gourgaud, A., like volcanism Bellon, H., 2007. Early Miocene adakite- in the Balkuyumcuregion, central Anatolia, Turkey: petrology and geochemistry. Journal of Asian Earth Sciences 30, 613–628.

105. Wang, Q., McDermott, F., Xu, J.F., Bellon, H., Zhu, Y.T., 2005. Cenozoic K-rich adakitic volcanic rocks in the Hohxil area, northern Tibet: lower-crustal melting in an intracontinental setting. Geology 33, 465–468.

106. Wang, Q., Wyman, A., Xu, J.F.,Wan, Y.S., Li, C.F., Zi, F., Jiang, Z.Q., Qiu, H.N., Chu, Z.Y., Zhao, Z.H., Dong, Y.H., 2008. Triassic Nb-enriched basalts, magnesian andesites, and adakites of the Qiangtang terrane (Central Tibet): evidence for metasomatism by slab-derived melts in the mantle wedge. Contrib. Mineral. Petrol. 155, 473–490.

107. Wang, Q., Wyman, D. A., Xu, J. F., Zhao, Z. H., Jian, P., Xiong, X. L., ... & Bai, Z. H. (2006). Petrogenesis of Cretaceous adakitic and shoshonitic igneous rocks in the Luzong area, Anhui Province (eastern China): implications for geodynamics and Cu–Au mineralization. Lithos, 89(3-4), 424-446.

108. Wang, Q., Wyman, D.A., Zhao, Z.H., Xu, Z.U., 2007. J., Bai, Z.H., Xiong, Z.H., Dai, T.M., Li, C.F., Chu, Petrogenesis of Carboniferous in adakites and Nb-enriched arc basalts the Alataw area, northern Tianshan Phanerozoic Range (western China): implications f or crustal growth In the 236, CentralAsia orogenic belt. Chemical Geology 42–64.

109. Wang, Q., Xu, J. F., Zhao, Z. H., Bao, Z. W., Xu, W., & Xiong, X. L. (2004). Cretaceous high-potassium intrusive rocks in the Yueshan-Hongzhen area of east China: Adakites in an extensional tectonic regime within a continent. Geochemical Journal, 38(5), 417-434.

110. Wen, D. R.; Chung, S. L.; Song, B.; Iizuka, Y.; Yang, H. J.; Ji, J. Q.; Liu, D. Y.; and Gallet, S. 2008. Late Cretaceous Gangdese intrusions of adakitic geochemical characteristics, SE Tibet: petrogenesis and tectonic implications. Lithos 105:1–11.

111. Xiangsong Wang, Min Sun, Roberto F. Weinberg, Keda Cai c, Guochun Zhao, Xiaoping Xia, Pengfei Li, Xijun Liu. Adakite generation as a result of fluid-fluxed melting at normal lower crustal pressures. Earth and Planetary Science Letters. Volume 594, 15 September 2022, 117744.

112. Xu, J., Shinjio, R., Defant, M.J., Wang, Q., Rapp, R.P., 2002. Origin of Mesozoic adakitic intrusive rocks in the Ningzhen area of east China: partial melting of delaminated lower continental crust? Geology 12, 1111–1114.

113. Yogodzinski, G.M., Kay, R.W., Volynets, nesian O.N., Koloskov, A.V., Kay, S.M., 1995. Mag-andesite in the western Aleutian Komandorsky region: implications for slab melting and processes in the mantle wedge. Geological Society of America Bulletin 107, 505–519.

114. Zack, T., Kronz, A., Foley, S.F., Rivers, T., 2002. Trace element abundances in retiles from eclogites and associated garnet mica schists. Chemical Geology 184, 97–122.

115. Zartman, R. E., & Doe, B. R. (1981). Plumbotectonics—the model. Tectonophysics, 75(1-2), 135-162.

116. Zartman, R. E., & Haines, S. M. (1988). The plumbotectonic model for Pb isotopic systematics among major terrestrial reservoirs—a case for bi-directional transport. Geochimica et cosmochimica acta, 52(6), 1327-1339.

117. Zindler, A., Hart, S.R., 1986. chemical geodynamics. Annual Review of Earth Planetary Sciences 14, 493–571.

 https://doi.org/10.5281/zenodo.14858968